

## Parameters of the Local Warp of the Stellar-Gaseous Galactic Disk from the Kinematics of Tycho-2 Nearby Red Giant Clump Stars

V.V. Bobylev

*Pulkovo Astronomical Observatory, Russian Academy of Sciences, St-Petersburg*

**Abstract**—We analyze the three-dimensional kinematics of about 82000 Tycho-2 stars belonging to the red giant clump (RGC). First, based on all of the currently available data, we have determined new, most probable components of the residual rotation vector of the optical realization of the ICRS/HIPPARCOS system relative to an inertial frame of reference,  $(\omega_x, \omega_y, \omega_z) = (-0.11, 0.24, -0.52) \pm (0.14, 0.10, 0.16)$  mas yr<sup>-1</sup>. The stellar proper motions in the form  $\mu_\alpha \cos \delta$  have then be corrected by applying the correction  $\omega_z = -0.52$  mas yr<sup>-1</sup>. We show that, apart from their involvement in the general Galactic rotation described by the Oort constants  $A = 15.82 \pm 0.21$  km s<sup>-1</sup> kpc<sup>-1</sup> and  $B = -10.87 \pm 0.15$  km s<sup>-1</sup> kpc<sup>-1</sup>, the RGC stars have kinematic peculiarities in the Galactic  $yz$  plane related to the kinematics of the warped stellar-gaseous Galactic disk. We show that the parameters of the linear Ogorodnikov–Milne model that describe the kinematics of RGC stars in the  $zx$  plane do not differ significantly from zero. The situation in the  $yz$  plane is different. For example, the component of the solid-body rotation vector of the local solar neighborhood around the Galactic  $x$  axis is  $M_{32}^- = -2.6 \pm 0.2$  km s<sup>-1</sup> kpc<sup>-1</sup>. Two parameters of the deformation tensor in this plane, namely  $M_{23}^+ = 1.0 \pm 0.2$  km s<sup>-1</sup> kpc<sup>-1</sup> and  $M_{33} - M_{22} = -1.3 \pm 0.4$  km s<sup>-1</sup> kpc<sup>-1</sup>, also differ significantly from zero. On the whole, the kinematics of the warped stellar-gaseous Galactic disk in the local solar neighborhood can be described as a rotation around the Galactic  $x$  axis (close to the line of nodes of this structure) with an angular velocity  $(-3.1 \pm 0.5) \leq \Omega_W \leq (-4.4 \pm 0.5)$  km s<sup>-1</sup> kpc<sup>-1</sup>.

## INTRODUCTION

Analysis of the large-scale structure of neutral hydrogen revealed a warp of the gaseous disk in the Galaxy (Westerhout 1957; Burton 1988). The results of studying this structure based on currently available data on the HI and HII distributions are presented in Kalberla and Dedes (2008) and Cersosimo et al. (2009), respectively. This structure is revealed by the spatial distribution of stars and dust (Drimmel and Spergel 2001), by the distribution of pulsars in the Galaxy (Yusifov 2004), by HIPPARCOS OB stars (Miyamoto and Zhu 1998), and by the 2MASS red giant clump (Momany et al. 2006).

Several models were suggested to explain the nature of the Galactic disk warp: (1) the interaction between the disk and a nonspherical dark matter halo (Sparke and Casertano 1988); (2) the gravitational influence of the Galaxy’s nearest satellites (Bailin 2003);

(3) the interaction of the disk with a near-Galaxy flow formed by high-velocity hydrogen clouds that resulted from mass exchange between the Galaxy and the Magellanic Clouds (Olano 2004); (4) an intergalactic flow (López-Corredoira et al. 2002); and (5) the interaction with the intergalactic magnetic field (Battaner et al. 1990).

By analyzing nearby stars from HIPPARCOS (1997), Dehnen (1998) showed that the distribution of their residual velocities in the  $V_y - V_z$  plane agreed satisfactorily with various rotation models of the warped disk. Miyamoto et al. (1993) and Miyamoto and Zhu (1998) determined the rotation parameters of the warped stellar–gaseous disk by analyzing giant stars of various spectral types and a sample of HIPPARCOS O–B5 stars. Thus, there is positive experience in solving this problem using data on stars relatively close to the Sun.

Studying the three-dimensional kinematics of stars requires that the observational data be free from the systematic errors related to the referencing of the optical realization of the ICRS/HIPPARCOS system to the inertial frame of reference specified by extragalactic sources. The modern standard system of astronomical coordinates, ICRS (International Celestial Reference System), is realized by the catalog of positions for 212 compact extragalactic radio sources uniformly distributed over the entire sky observed by the radio interferometry technique (Ma et al. 1998). In the optical range, the first realization of the ICRS was the HIPPARCOS catalog. The application of various methods of analysis shows that there is a small residual rotation of the ICRS/HIPPARCOS system relative to the inertial frame of reference with  $\omega_z \approx -0.4 \pm 0.1 \text{ mas yr}^{-1}$  (Bobylev 2004a, 2004b). At present, there are several new results of comparing individual programs with the catalogs of the ICRS/HIPPARCOS system. One of our goals is to determine the most probable components of the residual rotation vector of the optical realization of the ICRS/HIPPARCOS system relative to the inertial frame of reference.

The main goal of this paper is to study the local kinematics of the warped stellar–gaseous Galactic disk by analyzing the motions of Tycho-2 stars that belong to the red giant clump (RGC). Occupying a compact region on the Hertzsprung–Russell diagram, these stars are a kind of “standard candles”. Their estimated photometric distances are known with a mean accuracy of at least 20–30%. RGC stars are distributed uniformly in the spatial region and over the celestial sphere, which is an important property when the three-dimensional spatial motions of stars are analyzed.

## DATA

The characteristic clump, commonly called the red giant clump, on the Hertzsprung–Russell diagram is formed mostly by giants with masses from  $3M_\odot$  to  $9M_\odot$ . These stars spend the bulk of their lifetime on the main sequence as B-type stars. At the core helium burning stage, they evolve toward the RGC almost without changing their luminosity. At the RGC stage, despite the slow change in color, the luminosity of such a star remains almost constant. Therefore, RGC stars are convenient as “standard candles” for distance determinations. The RGC also incorporates other giants at different evolutionary stages. In addition, owing to probabilistic selection methods using reduced proper

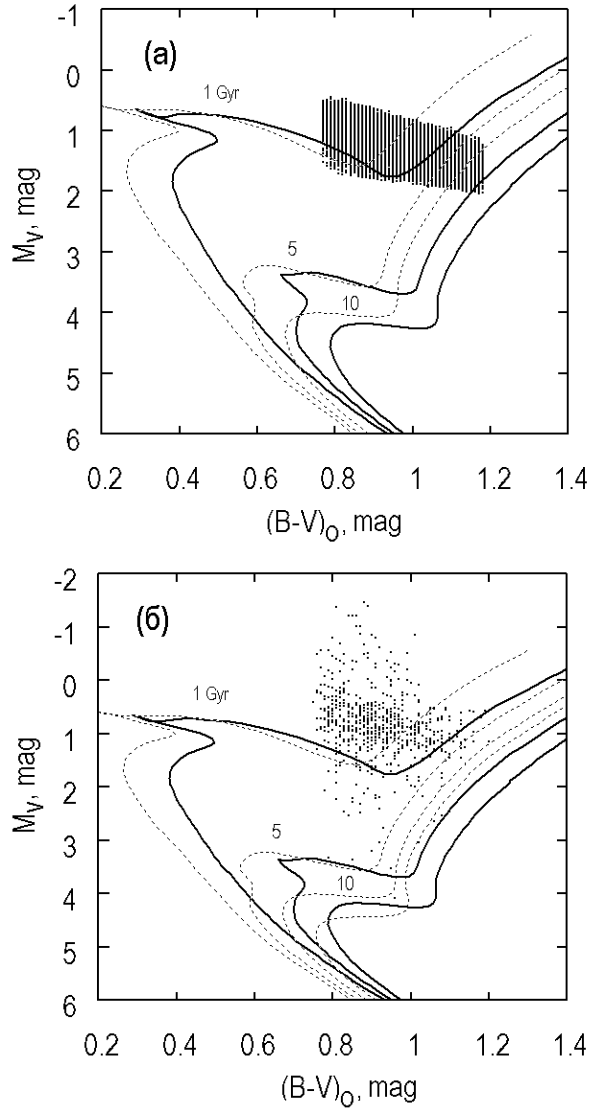


Fig. 1. Color–absolute magnitude diagram for 82324 RGC stars from the range of distances 0.3–1 kpc (a) and the sample of nearby RGC stars with reliable ( $e_\pi/\pi < 10\%$ ) HIPPARCOS parallaxes (b). The isochrones (Yi et al. 2003) for ages of 1, 5, and 10 Gyr with a nearly solar metallicity,  $Z = 0.02$  (dashed lines), and a higher metallicity,  $Z = 0.04$  (solid lines), are plotted.

motions, the RGC sample can be diluted by various stars from adjacent regions of the Hertzsprung–Russell diagram, both supergiants and dwarfs. According to the estimates by various authors, the admixture is small, may be 10–15% (Rybka 2006; Gontcharov 2008).

We used the list of 97000 RGC stars selected by Gontcharov (2008) by the dereddened color index and the reduced proper motion based on Tycho-2 (Hog et al. 2000) and 2MASS (Skrutskie et al. 2006) data. These stars occupy the region with  $0.^m5 < J - K_s < 0.^m9$  and  $-1.^m < M_{K_s} < -2.^m$  on the corresponding diagram. For their selection using the reduced proper motion, calibration based on HIPPARCOS stars with the most reliable data was performed. Details of the procedure are described in Gontcharov (2008). An estimate of the photometric distance and interstellar extinction is available for each star.

As was shown by Bobylev et al. (2009), the kinematic parameters of the Ogorodnikov–Milne model for relatively close ( $r < 0.2 - 0.3$  kpc) and distant ( $r > 1$  kpc) stars are determined with large errors when using the photometric distances of RGC stars. Therefore, here we use 82 324 stars from the range of distances  $0.3 \text{ kpc} < r < 1 \text{ kpc}$ , with the mean distance being  $r = 0.57 \pm 0.17$  kpc. To eliminate the halo stars from the sample, the following constraint on the proper motions was applied:  $\sqrt{(\mu_\alpha \cos \delta)^2 + (\mu_\delta)^2} < 300 \text{ mas yr}^{-1}$ .

As was shown by Bobylev et al. (2009), from a statistical analysis of the velocity dispersions, we found that about 20% of the RGC stars are very young, while an overwhelming majority of the remaining stars are characterized by the kinematics of thin-disk stars. We see from Fig. 1, where the color–absolute magnitude diagram is presented with a grid of isochrones with various ages and metallicities, that the RGC stars (Fig. 1a) are fairly young. Figure 1b presents about 650 stars from Gontcharov’s catalog selected as RGC ones with parallaxes from the HIPPARCOS catalog (with a parallax error of less than 10%). Although the segment of the isochrones near the RGC is very sensitive to metallicity, we clearly see from Fig. 1b that, first, the RGC stars proper have ages younger than 1 Gyr and, second, the admixture of dwarfs is insignificant.

## THE OGORODNIKOV–MILNE MODEL

We use a rectangular Galactic coordinate system with the axes directed away from the observer toward the Galactic center ( $l=0^\circ$ ,  $b=0^\circ$ , the  $X$  axis or axis 1), along the Galactic rotation ( $l=90^\circ$ ,  $b=0^\circ$ , the  $Y$  axis or axis 2), and toward the North Galactic Pole ( $b=90^\circ$ , the  $Z$  axis or axis 3).

In the linear Ogorodnikov–Milne model (Ogorodnikov, 1965), we use the notation introduced by Clube (1972, 1973) and used, for example, by Vityazev and Tsvetkov (2009).

The observed velocity  $\mathbf{V}(r)$  of a star with a heliocentric radius vector  $\mathbf{r}$ , is described, to the terms of the first order of smallness  $r/R_0 \ll 1$ , by the equation in vector form

$$\mathbf{V}(r) = \mathbf{V}_\odot + M\mathbf{r} + \mathbf{V}', \quad (1)$$

where  $\mathbf{V}_\odot(X_\odot, Y_\odot, Z_\odot)$  is the peculiar velocity of the Sun relative to the centroid of the

stars under consideration;  $\mathbf{V}'$  is the residual velocity of the star (here, the residual stellar velocities are assumed to have a random distribution);  $M$  is the displacement matrix (tensor) whose components are the partial derivatives of the velocity  $\mathbf{u}(u_1, u_2, u_3)$  with respect to the distance  $\mathbf{r}(r_1, r_2, r_3)$ , where  $\mathbf{u} = \mathbf{V}(R) - \mathbf{V}(R_0)$ , and  $R$  and  $R_0$  are the Galactocentric distances of the star and the Sun, respectively. Then,

$$M_{pq} = \left( \frac{\partial u_p}{\partial r_q} \right)_{\circ}, \quad (p, q = 1, 2, 3). \quad (2)$$

All nine elements of the matrix  $M$  can be determined using the three components of the observed velocities—the stellar radial velocities and proper motions. Having only the proper motions, we can write the conditional equations

$$4.74r\mu_l \cos b = X_{\odot} \sin l - Y_{\odot} \cos l + \quad (3)$$

$$+r[-\cos b \cos l \sin l M_{11} - \cos b \sin^2 l M_{12} - \sin b \sin l M_{13} + \cos b \cos^2 l M_{21} + \\ + \cos b \sin l \cos l M_{22} + \sin b \cos l M_{23}],$$

$$4.74r\mu_b = X_{\odot} \cos l \sin b + Y_{\odot} \sin l \sin b - Z_{\odot} \cos b + \quad (4)$$

$$+r[-\sin b \cos b \cos^2 l M_{11} - \sin b \cos b \sin l \cos l M_{12} - \\ - \sin^2 b \cos l M_{13} - \sin b \cos b \sin l \cos l M_{21} - \sin b \cos b \sin^2 l M_{22} - \sin^2 b \sin l M_{23} + \\ + \cos^2 b \cos l M_{31} + \cos^2 b \sin l M_{32} + \sin b \cos b M_{33}],$$

from which it follows that the terms should be grouped in several cases. It is useful to divide the matrix  $M$  into symmetric,  $M^+$  (local deformation tensor), and antisymmetric,  $M^-$  (rotation tensor), parts:

$$M_{pq}^+ = \frac{1}{2} \left( \frac{\partial u_p}{\partial r_q} + \frac{\partial u_q}{\partial r_p} \right)_{\circ}, \quad M_{pq}^- = \frac{1}{2} \left( \frac{\partial u_p}{\partial r_q} - \frac{\partial u_q}{\partial r_p} \right)_{\circ}, \quad (p, q = 1, 2, 3). \quad (5)$$

This allows the conditional equations to be written as

$$4.74r\mu_l \cos b = X_{\odot} \sin l - Y_{\odot} \cos l + \quad (6)$$

$$+r[-M_{32}^- \cos l \sin b - M_{13}^- \sin l \sin b + M_{21}^- \cos b + \\ + M_{12}^+ \cos 2l \cos b - M_{13}^+ \sin l \sin b + M_{23}^+ \cos l \sin b - 0.5(M_{11}^+ - M_{22}^+) \sin 2l \cos b],$$

$$4.74r\mu_b = X_{\odot} \cos l \sin b + Y_{\odot} \sin l \sin b - Z_{\odot} \cos b + \quad (7)$$

$$+r[M_{32}^- \sin l - M_{13}^- \cos l - 0.5M_{12}^+ \sin 2l \sin 2b + M_{13}^+ \cos l \cos 2b + \\ + M_{23}^+ \sin l \cos 2b - 0.5(M_{11}^+ - M_{22}^+) \cos^2 l \sin 2b + 0.5(M_{33}^+ - M_{22}^+) \sin 2b].$$

Equation (6) was obtained from Eq. (3) by adding two terms to its right-hand side,  $0.5M_{31}$  and  $0.5M_{32}$ , and subtracting them.

The system of equations (6) and (7) then becomes very convenient for its simultaneous solution. Indeed, as can be seen from Eq. (6), the two pairs of unknowns to be determined,  $M_{13}^-$  and  $M_{13}^+$ , along with  $M_{32}^-$  and  $M_{23}^+$ , have identical coefficients,  $\sin l \sin b$  and  $\cos l \sin b$ ,

respectively. In this case, the variables cannot be separated and can be found only from the simultaneous solution of the system of equations (6) and (7).

In addition, we see that one of the diagonal terms of the local deformation tensor remains uncertain. Therefore, we determine differences of the form  $(M_{11}^+ - M_{22}^+)$  and  $(M_{33}^+ - M_{22}^+)$ .

The quantities  $M_{32}^-, M_{13}^-, M_{12}^-$  are the components of the solid-body rotation vector of a small solar neighborhood around the  $x, y, z$  axes, respectively. According to our chosen rectangular coordinate system, the rotations from axis 1 to 2, from axis 2 to 3, and from axis 3 to 1 are positive.  $M_{21}^-$  is equivalent to the Oort constant  $B$ . Each of the quantities  $M_{12}^+, M_{13}^+, M_{23}^+$  describes the deformation in the corresponding plane.  $M_{12}^+$  is equivalent to the Oort constant  $A$ .

The diagonal components of the local deformation tensor  $M_{11}^+, M_{22}^+, M_{33}^+$  describe the general local contraction or expansion of the entire stellar system (divergence). The system of conditional equations (6) and (7) contain eleven unknowns to be determined by the least-squares method. In addition to the simultaneous solution of the system of equations (6) and (7), here we analyze the results of their separate solutions. In this case, Eq. (7) remains unchanged, while Eq. (6) is reduced to the form

$$\begin{aligned} 4.74r\mu_l \cos b = X_\odot \sin l - Y_\odot \cos l + \\ + r[M_{23} \cos l \sin b - M_{13} \sin l \sin b + M_{21}^- \cos b + M_{12}^+ \cos 2l \cos b - \\ - 0.5(M_{11}^+ - M_{22}^+) \sin 2l \cos b], \end{aligned} \quad (8)$$

where there are only seven independent variables.

## INERTIALITY OF THE OPTICAL ICRS/HIPPARCOS SYSTEM

Table 1 presents all of the currently known results of comparing individual programs with the catalogs of the ICRS/HIPPARCOS system.

First, we will briefly describe the results, most of which were used by Kovalevsky et al. (1997) to calibrate the HIPPARCOS catalog and to estimate its residual rotation relative to the system of extragalactic sources and by Bobylev (2004b) to solve this problem.

(1) The NPM1 solution. We used the result of comparing the stellar proper motions from the NPM1 (Klemola et al. 1994) and HIPPARCOS catalogs performed by the Heidelberg group (Kovalevsky et al. 1997). This solution was obtained in the range of magnitudes  $10^m.5$ – $11^m.5$ , where (Fig. 1 in Platais et al. 1998a) the HIPPARCOS–NPM1 stellar proper motion differences have a “horizontal” pattern near zero. In our opinion, the NPM1 proper motions in this magnitude range are free from the influence of the magnitude equation, which is significant in this catalog, to the greatest extent.

(2) The NPM2 solution. The stellar proper motions from the NPM2 and HIPPARCOS catalogs were compared by Zhu (2003). However, there are no images of galaxies on NPM2 photographic plates and, hence, these proper motions are relative. Therefore, we do not

Table 1: Components of the residual rotation vector of the optical realization of the ICRS/HIPPARCOS system relative to the inertial frame of reference

Method	$P_x/P_y/P_z$	$N_\star$	$N_{area}$	$\omega_x$ , mas yr $^{-1}$	$\omega_y$ , mas yr $^{-1}$	$\omega_z$ , mas yr $^{-1}$
NPM1	10/5/16	2616	899	$-0.76 \pm 0.25$	$+0.17 \pm 0.20$	$-0.85 \pm 0.20$
NPM2	(*)	3519	347	$-0.11 \pm 0.20$	$-0.19 \pm 0.20$	$-0.75 \pm 0.28$
SPM2	22/9/28	9356	156	$+0.10 \pm 0.17$	$+0.48 \pm 0.14$	$-0.17 \pm 0.15$
Kiev	1/1/1	415	154	$-0.27 \pm 0.80$	$+0.15 \pm 0.60$	$-1.07 \pm 0.80$
Potsdam	2/1/3	256	24	$+0.22 \pm 0.52$	$+0.43 \pm 0.50$	$+0.13 \pm 0.48$
Bonn	5/3/6	88	13	$+0.16 \pm 0.34$	$-0.32 \pm 0.25$	$+0.17 \pm 0.33$
HST	0.1/0.1/0.05	78		$-1.60 \pm 2.87$	$-1.92 \pm 1.54$	$+2.26 \pm 3.42$
EOP	8/2/—			$-0.93 \pm 0.28$	$-0.32 \pm 0.28$	—
PUL2	3/1/4	1004	147	$-0.98 \pm 0.47$	$-0.03 \pm 0.38$	$-1.66 \pm 0.42$
XPM	28/9/33	$1 \times 10^6$	1431	$-0.06 \pm 0.15$	$+0.17 \pm 0.14$	$-0.84 \pm 0.14$
VLBI-07	6/1/5	46		$-0.55 \pm 0.34$	$-0.02 \pm 0.36$	$+0.41 \pm 0.37$
Minor Pl	25/5/6	116		$+0.12 \pm 0.08$	$+0.66 \pm 0.09$	$-0.56 \pm 0.16$
Mean 1				$-0.22 \pm 0.19$	$+0.14 \pm 0.10$	$-0.49 \pm 0.23$
Mean 2				$-0.11 \pm 0.14$	$+0.24 \pm 0.10$	$-0.52 \pm 0.16$

Note. (\*)—the NPM2 solution is not used,  $N_\star$  is the number of stars/asteroids,  $N_{area}$  is the number of areas on the celestial sphere, mean 1 is a simple mean (without HST), mean 2 is a weighted mean.

use this solution to derive the mean values of  $\omega_x, \omega_y, \omega_z$ . It is given in Table 1 to emphasize its similarity to the NPM1 solution.

(3) The SPM2 solution. The stellar proper motions from the SPM2 (Platais et al. 1998b) and HIPPARCOS catalogs were compared by Zhu (2001).

(4) The PUL2 solution. The parameters  $\omega_x, \omega_y, \omega_z$  were found by comparing the Pulkovo PUL2 photographic catalog (Bobylov et al. 2004) and HIPPARCOS.

(5) The KIEV solution. The stellar proper motions from the GPM1 (Rybka and Yatsenko 1997) and HIPPARCOS catalogs were compared by Kislyuk et al. (1997).

(6) The POTSDAM solution. The parameters  $\omega_x, \omega_y, \omega_z$  of the Potsdam program were taken from Hirte et al. (1996).

(7) The BONN solution. The results of the Bonn program are presented in Geffert et al. (1997) and Tucholke et al. (1997).

(8) The EOP solution. The results of the analysis of Earth orientation parameters (EOP) were taken from Vondrák et al. (1997). Only two rotation parameters,  $\omega_x$ , and  $\omega_y$  are determined in this method.

(9) The HST solution. The results of stellar observations with the Hubble Space Telescope (HST) were taken from Hemenway et al. (1997).

Now, we will point out several new results that have not been used previously to solve this problem.

(10) The XPM solution. The XPM catalog (Fedorov et al., 2009) contains absolute proper motions for about 275 million stars fainter than 12m derived by comparing their positions in the 2MASS and USNO-A2.0 (Monet 1998) catalogs. The absolutization was made using about 1.5 million galaxies from the 2MASS catalog of extended sources. Thus, the XPM catalog is an independent realization of the inertial frame of reference. The stellar proper motions from the XPM and UCAC2 (Zacharias et al. 2004) catalogs were compared by Bobylev et al. (2010). The parameters  $\omega_x, \omega_y, \omega_z$  were calculated using about 1 million stars. Among all of the programs listed in Table 1, the XPM solution is unique in that it was obtained from the differences of stars covering the entire sky almost completely, except for the zone  $\delta > 54^\circ$ , where there are no UCAC2 stars.

(11) The VLBI-07 solution. Boboltz et al. (2007) analyzed the positions and proper motions of 46 radio stars and obtained new parameters of the mutual orientation of the optical realization (HIPPARCOS) and the radio system.

(12) The “MINOR PLANETS” solution. Chernetenko (2008) estimated the rotation parameters of the HIPPARCOS system relative to the DE403 and DE405 coordinate systems of ephemerides by analyzing a long-term series of asteroid observations. This result suggests that either the dynamical DE403 and DE405 theories need to be improved or the HIPPARCOS system needs to be corrected. We reduced the weight of this solution by half because of the possible contribution from the inaccuracy of the dynamical DE403 and DE405 theories.

The weight of each of the comparison catalogs was taken to be inversely proportional to the square of the random error  $e_\omega$  in the corresponding quantities  $\omega_x, \omega_y, \omega_z$  and was calculated from the formula

$$P_i = e_{kiev}^2 / e_i^2, \quad i = 1, \dots, 11. \quad (9)$$

Not all of the authors use the equations to determine  $\omega_x, \omega_y, \omega_z$  in the form in which they were suggested by Lindegren and Kovalevsky (1995):

$$\Delta\mu_\alpha \cos \delta = \omega_x \cos \alpha \sin \delta + \omega_y \sin \alpha \sin \delta - \omega_z \cos \delta, \quad (10)$$

$$\Delta\mu_\delta = -\omega_x \sin \alpha + \omega_y \cos \alpha, \quad (11)$$

where the catalog–HIPPARCOS differences are on the left-hand sides of the equations. Therefore, in several cases, the signs of the quoted quantities were reduced to the necessary uniform form (Zhu 2001, 2003; Boboltz et al. 2007).

The last rows of Table 1 give Mean 1 calculated as a simple mean and Mean 2 that was calculated as a weighted mean and is the main result of our analysis.

Denote the components of the rotation vector around the rectangular equatorial axes by  $\omega_x, \omega_y, \omega_z$ ; then,

$$\begin{pmatrix} \Omega_x \\ \Omega_y \\ \Omega_z \end{pmatrix} = \mathbf{G} \begin{pmatrix} M_{32}^- \\ M_{13}^- \\ M_{21}^- \end{pmatrix} + 4.74 \begin{pmatrix} \omega_x \\ \omega_y \\ -\omega_z \end{pmatrix}, \quad (12)$$



where

$$\mathbf{G} = \begin{pmatrix} -0.0548 & +0.4941 & -0.8677 \\ -0.8734 & -0.4448 & -0.1981 \\ -0.4838 & +0.7470 & +0.4560 \end{pmatrix} \quad (13)$$

is the well-known transformation matrix between the unit vectors of the Galactic and equatorial coordinate systems. From Eqs. (9) and (10), it is easy to see the relationship between  $M_{13}^-$  and  $\omega_z$ . Assuming the components in the mean-2 solution to be zero,

$$\begin{pmatrix} \Omega_x \\ \Omega_y \\ \Omega_z \end{pmatrix} = \mathbf{G} \begin{pmatrix} M_{32}^- \\ M_{13}^- \\ M_{21}^- \end{pmatrix} + 4.74 \begin{pmatrix} 0 \\ 0 \\ 0.52 \end{pmatrix}, \quad (14)$$

for the case where the left- and right-hand sides are expressed in  $\text{km s}^{-1} \text{ kpc}^{-1}$ .

## KINEMATICS OF THE DISK WARP

The results of determining the kinematic parameters of the Ogorodnikov–Milne model using a sample of RGC stars derived by simultaneously solving the system of equations (6) and (7) are presented in Table 2. The second column gives the solution obtained without applying any corrections to the input data; the third column gives the solution for the case where the stellar proper motions in the form  $\mu_\alpha \cos \delta$  were corrected by applying the correction  $\omega_z = -0.52 \text{ mas yr}^{-1}$  (14) using Eq. (10).

The parameters derived by separately solving Eqs. (8) and (7) are presented in Table 3.

As can be seen from Table 2, applying the correction affected only three components of the rotation tensor: insignificantly  $M_{21}^-$ , noticeably  $M_{32}^-$ , and most strongly  $M_{13}^-$ , which is explained by the structure of the matrix  $\mathbf{G}$  (13). Since the components  $M_{13}^-$  and  $M_{13}^+$  found (the third column of Table 2) do not differ significantly from zero, they may be set equal to zero.

Suppose that the values of  $M_{21}^-$  and  $M_{21}^+$  (the Oort constants) found describe only the rotation around the Galactic  $z$  axis, while the motion in the  $yz$  plane is independent. Let us now consider the displacement tensor  $M_W$  that describes the kinematics in the  $yz$  plane:

$$M_W = \begin{pmatrix} M_{22} & M_{23} \\ M_{32} & M_{33} \end{pmatrix} = \begin{pmatrix} \frac{\partial u_2}{\partial r_2} & \frac{\partial u_2}{\partial r_3} \\ \frac{\partial u_3}{\partial r_2} & \frac{\partial u_3}{\partial r_3} \end{pmatrix}. \quad (15)$$

As has already been noted, when using only the stellar proper motions, we can determine only the difference  $(M_{33}^+ - M_{22}^+)$ . The identity  $(M_{33}^+ - M_{22}^+) \equiv (M_{33} - M_{22})$  is valid for the diagonal elements. As can be seen from Table 2, the value of this quantity differs significantly from zero.

Three cases are possible when analyzing tensor (15):

- 1)  $M_{22} \neq 0, M_{33} = 0$ ;
- 2)  $M_{22} = 0, M_{33} \neq 0$ ;
- 3)  $M_{22} = 0, M_{33} = 0$ .

For the completeness of the picture, note that case 4 is also possible:  $M_{22} \neq 0, M_{33} \neq 0$ ; since this requires data on the stellar radial velocities, this case is not considered here.

Consider case 1,  $M_{33} = 0$ , using the data from the third column of Table 2,  $M_{22} = 1.3 \pm 0.4 \text{ km s}^{-1} \text{ kpc}^{-1}$ . The components of the displacement tensor  $M_W$ , the symmetric deformation tensor  $M_W^+$ , and the antisymmetric rotation tensor  $M_W^-$  are ( $\text{km s}^{-1} \text{ kpc}^{-1}$ )

$$M_W = \begin{pmatrix} 1.3_{(0.4)} & 3.6_{(0.3)} \\ -1.6_{(0.3)} & 0 \end{pmatrix}, \quad (16)$$

$$M_W^+ = \begin{pmatrix} 1.3_{(0.4)} & 1.0_{(0.2)} \\ 1.0_{(0.2)} & 0 \end{pmatrix}, \quad (17)$$

$$M_W^- = \begin{pmatrix} 0 & -2.6_{(0.2)} \\ -2.6_{(0.2)} & 0 \end{pmatrix}. \quad (18)$$

The deformation tensor  $M_W^+$  in the principal axes is ( $\text{km s}^{-1} \text{ kpc}^{-1}$ ):

$$\begin{aligned} M_W^+ &= \begin{pmatrix} \lambda_1 & 0 \\ 0 & \lambda_2 \end{pmatrix} = \\ &= \begin{pmatrix} 1.8 & 0 \\ 0 & -0.5 \end{pmatrix}, \end{aligned}$$

and the angle between the positive direction of the  $0y$  axis and the first principal axis of this ellipse is  $29 \pm 6^\circ$ .

Equation (1) can be written as

$$\mathbf{V} = \mathbf{V}_o + \text{grad } F + (\boldsymbol{\omega} \times \mathbf{r}).$$

Analysis of  $\text{grad } F$  shows (Sedov 1970) that an infinitesimal sphere of radius  $r$  composed of points of the medium at time  $t$ ,

$$x^2 + y^2 + z^2 = r^2$$

transforms into a deformation ellipsoid after time  $\Delta t$ ,

$$\frac{x^{*2}}{(1 + \lambda_1 \Delta t)^2} + \frac{y^{*2}}{(1 + \lambda_2 \Delta t)^2} + \frac{z^{*2}}{(1 + \lambda_3 \Delta t)^2} = r^2,$$

which is shown in Fig. 2b for our two-dimensional case.

For case 2, we have  $M_{33} = -1.3 \pm 0.4 \text{ km s}^{-1} \text{ kpc}^{-1}$  and  $M_{22} = 0$ . The deformation tensor  $M_W^+$  in the principal axes is ( $\text{km s}^{-1} \text{ kpc}^{-1}$ )

$$M_W^+ = \begin{pmatrix} 0.5 & 0 \\ 0 & -1.8 \end{pmatrix},$$

Table 2: Kinematic parameters of the Ogorodnikov–Milne model found by simultaneously solving the system of equations (6) and (7)

Parameter	Without correction	With correction
$X_{\odot}$	$7.99 \pm 0.10$	$7.99 \pm 0.10$
$Y_{\odot}$	$16.40 \pm 0.10$	$16.40 \pm 0.10$
$Z_{\odot}$	$6.72 \pm 0.09$	$6.72 \pm 0.09$
$A = M_{21}^+$	$15.82 \pm 0.21$	$15.82 \pm 0.21$
$M_{32}^-$	$-1.40 \pm 0.18$	$-2.60 \pm 0.18$
$M_{13}^-$	$-1.99 \pm 0.18$	$-0.15 \pm 0.18$
$B = M_{21}^-$	$-11.99 \pm 0.15$	$-10.87 \pm 0.15$
$M_{11-22}^+$	$-7.75 \pm 0.39$	$-7.75 \pm 0.39$
$M_{13}^+$	$-0.47 \pm 0.23$	$-0.47 \pm 0.23$
$M_{23}^+$	$1.00 \pm 0.22$	$1.00 \pm 0.22$
$M_{33-22}^+$	$-1.26 \pm 0.44$	$-1.26 \pm 0.44$

Note:  $X_{\odot}, Y_{\odot}, Z_{\odot}$  in  $\text{km s}^{-1}$ , other parameters in  $\text{km s}^{-1} \text{ kpc}^{-1}$ .

Table 3: Kinematic parameters of the Ogorodnikov–Milne model found by separately solving Eqs. (8) and (7)

Parameter	Without correction <sup>a</sup>	With correction <sup>a</sup>	Without correction <sup>b</sup>	With correction <sup>b</sup>
$X_{\odot}$	$7.89 \pm 0.12$	$7.89 \pm 0.12$	$8.51 \pm 0.21$	$8.51 \pm 0.21$
$Y_{\odot}$	$16.13 \pm 0.13$	$16.13 \pm 0.13$	$17.40 \pm 0.21$	$17.40 \pm 0.21$
$Z_{\odot}$	—	—	$6.73 \pm 0.08$	$6.73 \pm 0.08$
$A = M_{21}^+$	$15.76 \pm 0.25$	$15.76 \pm 0.25$	$15.99 \pm 0.48$	$15.99 \pm 0.48$
$M_{32}^-$	—	—	$-1.47 \pm 0.25$	$-2.66 \pm 0.25$
$M_{13}^-$	—	—	$-1.46 \pm 0.25$	$0.38 \pm 0.25$
$B = M_{21}^-$	$-12.02 \pm 0.17$	$-10.91 \pm 0.17$	—	—
$M_{11-22}^+$	$-8.21 \pm 0.46$	$-8.21 \pm 0.46$	$-4.31 \pm 1.03$	$-4.31 \pm 1.03$
$M_{13}^+$	—	—	$0.17 \pm 0.34$	$0.17 \pm 0.34$
$M_{23}^+$	—	—	$1.11 \pm 0.32$	$1.11 \pm 0.32$
$M_{33-22}^+$	—	—	$0.29 \pm 0.59$	$0.29 \pm 0.59$
$M_{23}$	$2.24 \pm 0.46$	$3.43 \pm 0.46$	—	—
$M_{13}$	$-2.93 \pm 0.43$	$-1.09 \pm 0.43$	—	—

<sup>a</sup>The parameters were found by solving Eq. (8).

<sup>b</sup>The parameters were found by solving Eq. (7).

Note:  $X_{\odot}, Y_{\odot}, Z_{\odot}$  in  $\text{km s}^{-1}$ , other parameters in  $\text{km s}^{-1} \text{ kpc}^{-1}$ .

the angle between the positive direction of the  $0y$  axis and the first principal axis of this ellipse is  $29 \pm 6^\circ$ .

For case 3, where  $M_{33} = 0$  and  $M_{22} = 0$ , the deformation tensor  $M_W^+$  has two roots:  $\lambda_1 = 1.0 \text{ km s}^{-1} \text{ kpc}^{-1}$  and  $\lambda_2 = -1.0 \text{ km s}^{-1} \text{ kpc}^{-1}$ ; therefore, the first principal axis of this ellipse is oriented at an angle of  $45^\circ$  to the  $0y$  axis.

In all three cases, the divergence  $0.5(M_{22} + M_{33})$  is insignificant. It is  $+0.6 \pm 0.4$ , and  $0 \text{ km s}^{-1} \text{ kpc}^{-1}$  for the first, second, and third cases, respectively.

As a result, we can conclude that the kinematics in the  $yz$  plane can be described as a rotation around the Galactic  $x$  axis with an angular velocity  $\Omega_W = M_{32}^- - \lambda_1$ . This angular velocity is  $-4.4 \pm 0.5$ ,  $-3.1 \pm 0.5$ , and  $-3.6 \pm 0.3 \text{ km s}^{-1} \text{ kpc}^{-1}$  for the first, second, and third cases, respectively.

Let us estimate the linear velocities in the  $yz$  plane. The mean photometric distance for our sample of RGC stars is  $\bar{r} = 0.57 \pm 0.17 \text{ kpc}$ . The linear solidbody rotation velocity is then  $M_{32}^- \cdot \bar{r} = -1.5 \pm 0.1 \text{ km s}^{-1}$ . The maximum deformation velocity is  $\lambda_1 \cdot \bar{r} = 1.0 \pm 0.3 \text{ km s}^{-1}$  and the highest (among the cases considered) linear velocity is  $\Omega_W \cdot \bar{r} = -2.5 \pm 0.3 \text{ km s}^{-1}$ .

Figure 2 gives a qualitative picture that reflects the pattern of our results. The distribution of rotation velocity vectors in the  $yz$  plane for the case of rotation we found is shown in Fig. 2a. Figure 2b shows how a circumference of unit radius turns into a deformation ellipse after a unit time interval.

According to the results of our separate solution of Eqs. (8) and (7) (the third and fifth columns of Table 3), for example, for case 1, we have

$$M_W = \begin{pmatrix} -0.3_{(0.6)} & 3.8_{(0.5)} \\ -1.6_{(0.4)} & 0 \end{pmatrix}, \quad (19)$$

$$M_W^+ = \begin{pmatrix} -0.3_{(0.6)} & 1.1_{(0.3)} \\ 1.1_{(0.3)} & 0 \end{pmatrix}, \quad (20)$$

$$M_W^- = \begin{pmatrix} 0 & -2.7_{(0.3)} \\ -2.7_{(0.3)} & 0 \end{pmatrix}. \quad (21)$$

We can see from our comparison of matrixes (19) and (16), (20) and (17), (21) and (18) that there are differences only in the diagonal element. This leads us to conclude that both approaches used (the simultaneous and separate solution of the equations) are equivalent, because they yield coincident results.

When writing Eq. (14), we set the components equal to zero,  $\omega_x = 0$  and  $\omega_y = 0$ . As we see from the Mean 2 solution in Table 1, the value of the component  $\omega_y$  was found to be nonzero outside the  $2\sigma$  range. However, the kinematic parameters calculated by taking this into account, i.e.,  $\omega_y \neq 0$  and  $\omega_z \neq 0$ , have no significant differences between the solutions reflected in Tables 2 and 3 and, hence, we do not give them.

## DISCUSSION

Drimmel et al. (2000) provide arguments for the model of precession of the warped disk in the  $zx$  plane (rotation around the  $y$  axis) with an angular velocity of  $-25 \text{ km s}^{-1} \text{ kpc}^{-1}$ .

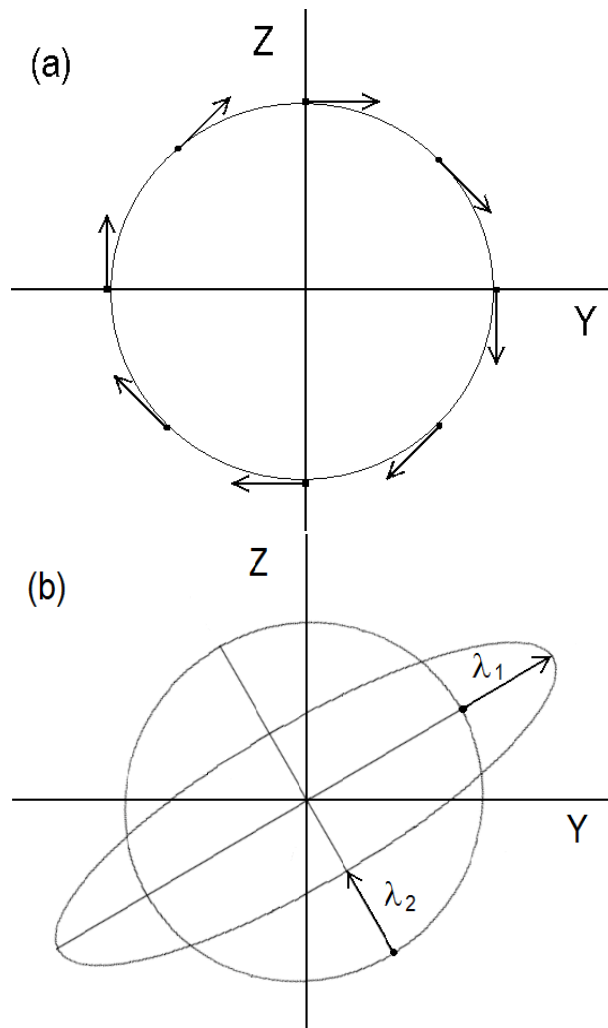


Fig. 2. Distribution of rotation velocity vectors (a) and deformation velocity vectors (b) in the  $yz$  plane.

However, as can be seen from Table 2, as a result of applying the correction  $\omega_z = -0.52$  mas yr<sup>-1</sup>, the component of the rotation tensor around the  $y$  axis ( $M_{13}^-$ ) has an almost zero value and the component of the deformation tensor in this plane ( $M_{13}^+$ ) does not differ significantly from zero.

The angular velocity  $\Omega_W$  estimated here is inconsistent with the analysis of the motion of giants of various spectral types (O–M) performed by Miyamoto et al. (1993), who found a positive direction of rotation around the  $x$  axis (directed toward the Galactic center). Note that the analyzed stellar proper motions were determined in the FK5 (Fundamental Catalog 5) system, which is noticeably distorted by the uncertainty in the precession constant. On the other hand, having analyzed the proper motions of O–B5 stars in the HIPPARCOS system, Miyamoto and Zhu (1998) also reached the conclusion about a positive rotation around the  $x$  axis.

At present, it is impossible to choose between the three forms of the deformation tensor considered in the previous section due to the absence of data on stellar radial velocities and distances. Note that based on a sample of 3632 relatively close RGC stars with known HIPPARCOS trigonometric parallaxes and radial velocities, we estimated the parameters  $M_{22} = -1.3 \pm 3.2$  km s<sup>-1</sup> kpc<sup>-1</sup> and  $M_{33} = -1.1 \pm 2.6$  km s<sup>-1</sup> kpc<sup>-1</sup> (Bobylev et al. 2009). Consequently, the difference ( $M_{33}^+ - M_{22}^+$ ) is very close to zero and, hence, the orientation of the deformation ellipse is close to 45°, as in case 3 considered.

In the Introduction, we listed various hypotheses about the nature of the Galactic disk warp. In our opinion, the hypothesis about an outflow of gas from the Magellanic Clouds (Olano 2004) has been worked out in greatest detail. Assuming the distance to the Large Magellanic Cloud to be  $r_{LMC} = 50$  kpc, we find that the linear velocity of the rotation we revealed at this distance,  $(-3.1 \pm 0.5) \leq \Omega_W \leq (-4.4 \pm 0.5)$  km s<sup>-1</sup> kpc<sup>-1</sup>, is  $|\Omega_W| \cdot r_{LMC} = (155 \div 220) \pm 25$  km s<sup>-1</sup>. Such velocities are in agreement with the estimate of the motion of high-velocity hydrogen clouds relative to the local standard of rest,  $\approx 200$  km s<sup>-1</sup> (Olano 2004), and the rotation direction we found is in good agreement with the direction of motion of the Magellanic Clouds around the Galaxy during the past 570 Myr (Fig. 6 from Olano 2004).

## CONCLUSIONS

We analyzed the kinematics of about 82000 RGC stars from the Tycho-2 catalog. These stars are a variety of “standard candles”, because they occupy a compact region on the Hertzsprung-Russell diagram. Therefore, photometric distance estimates with an accuracy of at least 30% are available for them. The RGC stars considered lie in the range of heliocentric distances  $0.3 \text{ kpc} < d < 1 \text{ kpc}$ .

Since these stars are distributed fairly uniformly in space, they are of great interest not only in studying the Galaxy’s general rotation described by the rotation parameters in the Galactic  $xy$  plane but also in the other two planes, namely  $yz$  and  $zx$ .

For a reliable description of their kinematic peculiarities, we should be confident that the observational data (Tycho-2 proper motions) are free from the systematic errors related to the referencing of the optical realization of the ICRS/HIPPARCOS system to the

inertial frame of reference specified by extragalactic sources.

Here, we gave much attention to this problem. Based on all of the currently available data, we determined new, most probable components of the residual rotation vector of the optical realization of the ICRS/HIPPARCOS system relative to the inertial frame of reference,  $(\omega_x, \omega_y, \omega_z) = (-0.11, 0.24, -0.52) \pm (0.14, 0.10, 0.16) \text{ mas yr}^{-1}$ . This led us to conclude that a small correction,  $\omega_z = -0.52 \text{ mas yr}^{-1}$ , should be applied to the Tycho-2 stellar proper motions of the form  $\mu_\alpha \cos \delta$ .

By applying this correction, we showed that, apart from their involvement in the general Galactic rotation described by the Oort constants  $A = 15.8 \pm 0.2 \text{ km s}^{-1} \text{ kpc}^{-1}$  and  $B = -10.9 \pm 0.2 \text{ km s}^{-1} \text{ kpc}^{-1}$ , the RGC stars considered have peculiarities in the  $yz$  plane related, in our opinion, to the kinematics of the warped Galactic stellar-gaseous disk.

The component of the solid-body rotation of the local solar neighborhood around the Galactic  $x$  axis is  $M_{32}^- = -2.6 \pm 0.2 \text{ km s}^{-1} \text{ kpc}^{-1}$ . The parameter of the deformation tensor in this plane  $M_{23}^+ = 1.0 \pm 0.2 \text{ km s}^{-1} \text{ kpc}^{-1}$  and the difference  $M_{33} - M_{22} = -1.3 \pm 0.4 \text{ km s}^{-1} \text{ kpc}^{-1}$  differ significantly from zero.

On the whole, the kinematics of the warped Galactic stellar-gaseous disk in the local solar neighborhood can be described as a rotation around the Galactic  $x$  axis directed from the Sun toward the Galactic center with an angular velocity  $(-3.1 \pm 0.5) \leq \Omega_W \leq (-4.4 \pm 0.5) \text{ km s}^{-1} \text{ kpc}^{-1}$ . Thus, the rotation is around an axis close to the line of nodes of this structure. In the case where the difference  $M_{33} - M_{22}$  may be set equal to zero, the angular velocity  $\Omega_W$  is  $-3.6 \pm 0.3 \text{ km s}^{-1} \text{ kpc}^{-1}$ . If  $M_{22} = 0$  and  $M_{33} \neq 0$ , then  $\Omega_W = -3.1 \pm 0.5 \text{ km s}^{-1} \text{ kpc}^{-1}$ . If  $M_{22} \neq 0$  and  $M_{33} = 0$ , then  $\Omega_W$  reaches  $-4.4 \pm 0.5 \text{ km s}^{-1} \text{ kpc}^{-1}$ .

## ACKNOWLEDGMENTS

I am grateful to the referees for helpful remarks that contributed to an improvement of the paper and to A.T. Bajkova for her help in the work. This study was supported by the Russian Foundation for Basic Research (project nos. 08-02-00400 and 09-02-90443-Ukr-f) and, in part, by the ‘‘Origin and Evolution of Stars and Galaxies’’ Program of the Presidium of the Russian Academy of Sciences.

## REFERENCES

1. J. Bailin, *Astrophys. J.* 583, L79 (2003).
2. E. Battaner, E. Florido, and M.L. Sanchez-Saavedra, *Astron. Astrophys.* 236, 1 (1990).
3. D.A. Boboltz, A.L. Fey, W.K. Puatua, et al., *Astron. J.* 133, 906 (2007).
4. V.V. Bobylev, *Pis'ma Astron. Zh.* 30, 289 (2004a) [*Astron. Lett.* 30, 251 (2004)].
5. V.V. Bobylev, *Pis'ma Astron. Zh.* 30, 930 (2004b) [*Astron. Lett.* 30, 848 (2004)].
6. V.V. Bobylev, N.M. Bronnikova, and N.A. Shakht, *Pis'ma Astron. Zh.* 30, 519 (2004) [*Astron. Lett.* 30, 469 (2004)].

7. V.V. Bobylev, A.S. Stepanishchev, A.T. Bajkova, and G.A. Gontcharov, *Pis'ma Astron. Zh.* 35, 920 (2009) [*Astron. Lett.* 35, 836 (2009)].
8. V.V. Bobylev, P.N. Fedorov, A.T. Bajkova, and V.S. Akhmetov, *Pis'ma Astron. Zh.* 36, 535 (2010) [*Astron. Lett.* 36, 506 (2010)].
9. W.B. Burton, *Galactic and Extragalactic Radio Astronomy*, Ed. by G. Verschuur and K. Kellerman (Springer, New York, 1988), p. 295.
10. J.C. Cersosimo, S. Mader, N. Santiago Figueroa, et al., *Astrophys. J.* 699, 469 (2009).
11. Yu.A. Chernetenko, *Pis'ma Astron. Zh.* 34, 296 (2008) [*Astron. Lett.* 34, 266 (2008)].
12. S.V.M. Clube, *Mon. Not. R. Astron. Soc.* 159, 289 (1972).
13. S.V.M. Clube, *Mon. Not. R. Astron. Soc.* 161, 445 (1973).
14. W. Dehnen, *Astron. J.* 115, 2384 (1998).
15. R. Drimmel and D.N. Spergel, *Astrophys. J.* 556, 181 (2001).
16. R. Drimmel, R.L. Smart, and M.G. Lattanzi, *Astron. Astrophys.* 354, 67 (2000).
17. P.N. Fedorov, A.A. Myznikov, and V.S. Akhmetov, *Mon. Not. R. Astron. Soc.* 393, 133 (2009).
18. M. Geffert, A.R. Klemola, M. Hiesgen, et al., *Astron. Astrophys.* 124, 157 (1997).
19. G.A. Gontcharov, *Pis'ma Astron. Zh.* 34, 868 (2008) [*Astron. Lett.* 34, 785 (2008)].
20. P.D. Hemenway, R.L. Duncombe, E.P. Bozayan, et al., *Astron. J.* 114, 2796 (1997).
21. *The HIPPARCOS and Tycho Catalogues*, ESA SP-1200 (1997).
22. S. Hirte, E. Schilbach, and R.-D. Scholz, *Astron. Astrophys. Suppl. Ser.* 126, 31 (1996).
23. E. Hog, C. Fabricius, V.V. Makarov, et al., *Astron. Astrophys.* 355, L27 (2000).
24. P.M.W. Kalberla and L. Dedes, *Astron. Astrophys.* 487, 951 (2008).
25. V.S. Kislyuk, SP. Rybka, A.I. Yatsenko, et al., *Astron. Astrophys.* 321, 660 (1997).
26. A.R. Klemola, R.B. Hanson, and B.F. Jones, in *Galactic and Solar System Optical Astrometry*, Ed. by L.V. Morrison and G.F. Gilmore (Cambridge Univ., Cambridge, 1994), p. 20.
27. J. Kovalevsky, L. Lindegren, M.A.C. Perryman, et al., *Astron. Astrophys.* 323, 620 (1997).
28. L. Lindegren and J. Kovalevsky, *Astron. Astrophys.* 304, 189 (1995).
29. M. López-Corredoira, J. Betancort-Rijo, and J. Beckman, *Astron. Astrophys.* 386, 169 (2002).
30. C. Ma, E.F. Arias, T.M. Eubanks, et al., *Astron. J.* 116, 516 (1998).
31. M. Miyamoto and Z. Zhu, *Astron. J.* 115, 1483 (1998).
32. M. Miyamoto, M. Sôma, and M. Yoshizawa, *Astron. J.* 105, 2138 (1993).
33. Y. Momany, S. Zaggia, G. Gilmore, et al., *Astron. Astrophys.* 451, 515 (2006).
34. D.G. Monet, *Bull. Am. Astron. Soc.* 30, 1427 (1998).
35. K.F. Ogorodnikov, *Dynamics of Stellar Systems* (Fizmatgiz, Moscow, 1965) [in Russian].



36. C.A. Olano, *Astron. Astrophys.* 423, 895 (2004).
37. I. Platais, V. Kozhurina-Platais, T.M. Girard, et al., *Astron. Astrophys.* 331, 1119 (1998a).
38. I. Platais, T.M. Girard, V. Kozhurina-Platais, et al., *Astron. J.* 116, 2556 (1998b).
39. S.P. Rybka, *Kinem Fiz. Neb. Tel* 22, 225 (2006).
40. S.P. Rybka and A.I. Yatsenko, *Astron. Astrophys. Suppl. Ser.* 121, 243 (1997).
41. L.I. Sedov, *Mechanics of Continuous Media* (Nauka, Moscow, 1970), Vol. 1 [in Russian].
42. M.F. Skrutskie, R.M. Cutri, R. Stiening, et al., *Astron. J.* 131, 1163 (2006).
43. L. Sparke and S. Casertano, *Mon. Not. R. Astron. Soc.* 234, 873 (1988).
44. H.-J. Tucholke, P. Brosche, and M. Odenkirchen, *Astron. Astrophys. Suppl. Ser.* 124, 157 (1997).
45. V.V. Vityazev and A.S. Tsvetkov, *Pis'ma Astron. Zh.* 35, 114 (2009) [*Astron. Lett.* 35, 100 (2009)].
46. J. Vondrák, C. Ron, I. Pešek, *Astron. Astrophys.* 319, 1020 (1997).
47. G. Westerhout, *Bull. Astron. Inst. Netherlands* 13, 201 (1957).
48. S.K. Yi, Y.-C. Kim, and P. Demarque, *Astrophys. J. Suppl. Ser.* 144, 259 (2003).
49. I. Yusifov, *astro-ph/0405517* (2004).
50. N. Zacharias, S.E. Urban, M.I. Zacharias, et al., *Astron. J.* 127, 3043 (2004).
51. Zi Zhu, *Publ. Astron. Soc. Jpn.* 53, L33 (2001).
52. Zi Zhu, in *JOURNEÉS-2003, Astrometry, Geodynamics and Solar System Dynamics: From Milliarcseconds to Microarcseconds*, Ed. by N. Capitaine (Observ. de Paris, Paris, 2003), p. 95.

Translated by N. Samus'

## Parameters of the Local Warp of the Stellar-Gaseous Galactic Disk from the Kinematics of Tycho-2 Nearby Red Giant Clump Stars

V.V. Bobylev

*Pulkovo Astronomical Observatory, Russian Academy of Sciences, St-Petersburg*

**Abstract**—We analyze the three-dimensional kinematics of about 82000 Tycho-2 stars belonging to the red giant clump (RGC). First, based on all of the currently available data, we have determined new, most probable components of the residual rotation vector of the optical realization of the ICRS/HIPPARCOS system relative to an inertial frame of reference,  $(\omega_x, \omega_y, \omega_z) = (-0.11, 0.24, -0.52) \pm (0.14, 0.10, 0.16)$  mas yr<sup>-1</sup>. The stellar proper motions in the form  $\mu_\alpha \cos \delta$  have then be corrected by applying the correction  $\omega_z = -0.52$  mas yr<sup>-1</sup>. We show that, apart from their involvement in the general Galactic rotation described by the Oort constants  $A = 15.82 \pm 0.21$  km s<sup>-1</sup> kpc<sup>-1</sup> and  $B = -10.87 \pm 0.15$  km s<sup>-1</sup> kpc<sup>-1</sup>, the RGC stars have kinematic peculiarities in the Galactic  $yz$  plane related to the kinematics of the warped stellar-gaseous Galactic disk. We show that the parameters of the linear Ogorodnikov–Milne model that describe the kinematics of RGC stars in the  $zx$  plane do not differ significantly from zero. The situation in the  $yz$  plane is different. For example, the component of the solid-body rotation vector of the local solar neighborhood around the Galactic  $x$  axis is  $M_{32}^- = -2.6 \pm 0.2$  km s<sup>-1</sup> kpc<sup>-1</sup>. Two parameters of the deformation tensor in this plane, namely  $M_{23}^+ = 1.0 \pm 0.2$  km s<sup>-1</sup> kpc<sup>-1</sup> and  $M_{33} - M_{22} = -1.3 \pm 0.4$  km s<sup>-1</sup> kpc<sup>-1</sup>, also differ significantly from zero. On the whole, the kinematics of the warped stellar-gaseous Galactic disk in the local solar neighborhood can be described as a rotation around the Galactic  $x$  axis (close to the line of nodes of this structure) with an angular velocity  $(-3.1 \pm 0.5) \leq \Omega_W \leq (-4.4 \pm 0.5)$  km s<sup>-1</sup> kpc<sup>-1</sup>.

## INTRODUCTION

Analysis of the large-scale structure of neutral hydrogen revealed a warp of the gaseous disk in the Galaxy (Westerhout 1957; Burton 1988). The results of studying this structure based on currently available data on the HI and HII distributions are presented in Kalberla and Dedes (2008) and Cersosimo et al. (2009), respectively. This structure is revealed by the spatial distribution of stars and dust (Drimmel and Spergel 2001), by the distribution of pulsars in the Galaxy (Yusifov 2004), by HIPPARCOS OB stars (Miyamoto and Zhu 1998), and by the 2MASS red giant clump (Momany et al. 2006).

Several models were suggested to explain the nature of the Galactic disk warp: (1) the interaction between the disk and a nonspherical dark matter halo (Sparke and Casertano 1988); (2) the gravitational influence of the Galaxy’s nearest satellites (Bailin 2003);

(3) the interaction of the disk with a near-Galaxy flow formed by high-velocity hydrogen clouds that resulted from mass exchange between the Galaxy and the Magellanic Clouds (Olano 2004); (4) an intergalactic flow (López-Corredoira et al. 2002); and (5) the interaction with the intergalactic magnetic field (Battaner et al. 1990).

By analyzing nearby stars from HIPPARCOS (1997), Dehnen (1998) showed that the distribution of their residual velocities in the  $V_y - V_z$  plane agreed satisfactorily with various rotation models of the warped disk. Miyamoto et al. (1993) and Miyamoto and Zhu (1998) determined the rotation parameters of the warped stellar–gaseous disk by analyzing giant stars of various spectral types and a sample of HIPPARCOS O–B5 stars. Thus, there is positive experience in solving this problem using data on stars relatively close to the Sun.

Studying the three-dimensional kinematics of stars requires that the observational data be free from the systematic errors related to the referencing of the optical realization of the ICRS/HIPPARCOS system to the inertial frame of reference specified by extragalactic sources. The modern standard system of astronomical coordinates, ICRS (International Celestial Reference System), is realized by the catalog of positions for 212 compact extragalactic radio sources uniformly distributed over the entire sky observed by the radio interferometry technique (Ma et al. 1998). In the optical range, the first realization of the ICRS was the HIPPARCOS catalog. The application of various methods of analysis shows that there is a small residual rotation of the ICRS/HIPPARCOS system relative to the inertial frame of reference with  $\omega_z \approx -0.4 \pm 0.1 \text{ mas yr}^{-1}$  (Bobylev 2004a, 2004b). At present, there are several new results of comparing individual programs with the catalogs of the ICRS/HIPPARCOS system. One of our goals is to determine the most probable components of the residual rotation vector of the optical realization of the ICRS/HIPPARCOS system relative to the inertial frame of reference.

The main goal of this paper is to study the local kinematics of the warped stellar–gaseous Galactic disk by analyzing the motions of Tycho-2 stars that belong to the red giant clump (RGC). Occupying a compact region on the Hertzsprung–Russell diagram, these stars are a kind of “standard candles”. Their estimated photometric distances are known with a mean accuracy of at least 20–30%. RGC stars are distributed uniformly in the spatial region and over the celestial sphere, which is an important property when the three-dimensional spatial motions of stars are analyzed.

## DATA

The characteristic clump, commonly called the red giant clump, on the Hertzsprung–Russell diagram is formed mostly by giants with masses from  $3M_\odot$  to  $9M_\odot$ . These stars spend the bulk of their lifetime on the main sequence as B-type stars. At the core helium burning stage, they evolve toward the RGC almost without changing their luminosity. At the RGC stage, despite the slow change in color, the luminosity of such a star remains almost constant. Therefore, RGC stars are convenient as “standard candles” for distance determinations. The RGC also incorporates other giants at different evolutionary stages. In addition, owing to probabilistic selection methods using reduced proper

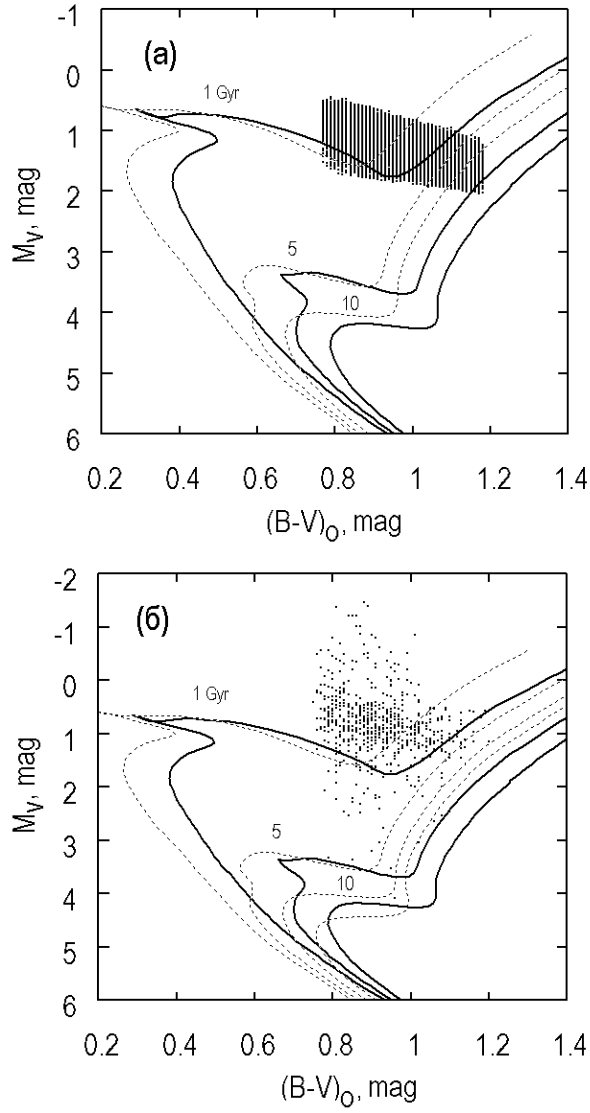


Fig. 1. Color–absolute magnitude diagram for 82324 RGC stars from the range of distances 0.3–1 kpc (a) and the sample of nearby RGC stars with reliable ( $e_\pi/\pi < 10\%$ ) HIPPARCOS parallaxes (b). The isochrones (Yi et al. 2003) for ages of 1, 5, and 10 Gyr with a nearly solar metallicity,  $Z = 0.02$  (dashed lines), and a higher metallicity,  $Z = 0.04$  (solid lines), are plotted.

motions, the RGC sample can be diluted by various stars from adjacent regions of the Hertzsprung–Russell diagram, both supergiants and dwarfs. According to the estimates by various authors, the admixture is small, may be 10–15% (Rybka 2006; Gontcharov 2008).

We used the list of 97000 RGC stars selected by Gontcharov (2008) by the dereddened color index and the reduced proper motion based on Tycho-2 (Hog et al. 2000) and 2MASS (Skrutskie et al. 2006) data. These stars occupy the region with  $0.^m5 < J - K_s < 0.^m9$  and  $-1.^m < M_{K_s} < -2.^m$  on the corresponding diagram. For their selection using the reduced proper motion, calibration based on HIPPARCOS stars with the most reliable data was performed. Details of the procedure are described in Gontcharov (2008). An estimate of the photometric distance and interstellar extinction is available for each star.

As was shown by Bobylev et al. (2009), the kinematic parameters of the Ogorodnikov–Milne model for relatively close ( $r < 0.2 - 0.3$  kpc) and distant ( $r > 1$  kpc) stars are determined with large errors when using the photometric distances of RGC stars. Therefore, here we use 82 324 stars from the range of distances  $0.3 \text{ kpc} < r < 1 \text{ kpc}$ , with the mean distance being  $r = 0.57 \pm 0.17$  kpc. To eliminate the halo stars from the sample, the following constraint on the proper motions was applied:  $\sqrt{(\mu_\alpha \cos \delta)^2 + (\mu_\delta)^2} < 300 \text{ mas yr}^{-1}$ .

As was shown by Bobylev et al. (2009), from a statistical analysis of the velocity dispersions, we found that about 20% of the RGC stars are very young, while an overwhelming majority of the remaining stars are characterized by the kinematics of thin-disk stars. We see from Fig. 1, where the color–absolute magnitude diagram is presented with a grid of isochrones with various ages and metallicities, that the RGC stars (Fig. 1a) are fairly young. Figure 1b presents about 650 stars from Gontcharov’s catalog selected as RGC ones with parallaxes from the HIPPARCOS catalog (with a parallax error of less than 10%). Although the segment of the isochrones near the RGC is very sensitive to metallicity, we clearly see from Fig. 1b that, first, the RGC stars proper have ages younger than 1 Gyr and, second, the admixture of dwarfs is insignificant.

## THE OGORODNIKOV–MILNE MODEL

We use a rectangular Galactic coordinate system with the axes directed away from the observer toward the Galactic center ( $l=0^\circ$ ,  $b=0^\circ$ , the  $X$  axis or axis 1), along the Galactic rotation ( $l=90^\circ$ ,  $b=0^\circ$ , the  $Y$  axis or axis 2), and toward the North Galactic Pole ( $b=90^\circ$ , the  $Z$  axis or axis 3).

In the linear Ogorodnikov–Milne model (Ogorodnikov, 1965), we use the notation introduced by Clube (1972, 1973) and used, for example, by Vityazev and Tsvetkov (2009).

The observed velocity  $\mathbf{V}(r)$  of a star with a heliocentric radius vector  $\mathbf{r}$ , is described, to the terms of the first order of smallness  $r/R_0 \ll 1$ , by the equation in vector form

$$\mathbf{V}(r) = \mathbf{V}_\odot + M\mathbf{r} + \mathbf{V}', \quad (1)$$

where  $\mathbf{V}_\odot(X_\odot, Y_\odot, Z_\odot)$  is the peculiar velocity of the Sun relative to the centroid of the

stars under consideration;  $\mathbf{V}'$  is the residual velocity of the star (here, the residual stellar velocities are assumed to have a random distribution);  $M$  is the displacement matrix (tensor) whose components are the partial derivatives of the velocity  $\mathbf{u}(u_1, u_2, u_3)$  with respect to the distance  $\mathbf{r}(r_1, r_2, r_3)$ , where  $\mathbf{u} = \mathbf{V}(R) - \mathbf{V}(R_0)$ , and  $R$  and  $R_0$  are the Galactocentric distances of the star and the Sun, respectively. Then,

$$M_{pq} = \left( \frac{\partial u_p}{\partial r_q} \right)_{\circ}, \quad (p, q = 1, 2, 3). \quad (2)$$

All nine elements of the matrix  $M$  can be determined using the three components of the observed velocities—the stellar radial velocities and proper motions. Having only the proper motions, we can write the conditional equations

$$4.74r\mu_l \cos b = X_{\odot} \sin l - Y_{\odot} \cos l + \quad (3)$$

$$+r[-\cos b \cos l \sin l M_{11} - \cos b \sin^2 l M_{12} - \sin b \sin l M_{13} + \cos b \cos^2 l M_{21} + \\ + \cos b \sin l \cos l M_{22} + \sin b \cos l M_{23}],$$

$$4.74r\mu_b = X_{\odot} \cos l \sin b + Y_{\odot} \sin l \sin b - Z_{\odot} \cos b + \quad (4)$$

$$+r[-\sin b \cos b \cos^2 l M_{11} - \sin b \cos b \sin l \cos l M_{12} - \\ - \sin^2 b \cos l M_{13} - \sin b \cos b \sin l \cos l M_{21} - \sin b \cos b \sin^2 l M_{22} - \sin^2 b \sin l M_{23} + \\ + \cos^2 b \cos l M_{31} + \cos^2 b \sin l M_{32} + \sin b \cos b M_{33}],$$

from which it follows that the terms should be grouped in several cases. It is useful to divide the matrix  $M$  into symmetric,  $M^+$  (local deformation tensor), and antisymmetric,  $M^-$  (rotation tensor), parts:

$$M_{pq}^+ = \frac{1}{2} \left( \frac{\partial u_p}{\partial r_q} + \frac{\partial u_q}{\partial r_p} \right)_{\circ}, \quad M_{pq}^- = \frac{1}{2} \left( \frac{\partial u_p}{\partial r_q} - \frac{\partial u_q}{\partial r_p} \right)_{\circ}, \quad (p, q = 1, 2, 3). \quad (5)$$

This allows the conditional equations to be written as

$$4.74r\mu_l \cos b = X_{\odot} \sin l - Y_{\odot} \cos l + \quad (6)$$

$$+r[-M_{32}^- \cos l \sin b - M_{13}^- \sin l \sin b + M_{21}^- \cos b + \\ + M_{12}^+ \cos 2l \cos b - M_{13}^+ \sin l \sin b + M_{23}^+ \cos l \sin b - 0.5(M_{11}^+ - M_{22}^+) \sin 2l \cos b],$$

$$4.74r\mu_b = X_{\odot} \cos l \sin b + Y_{\odot} \sin l \sin b - Z_{\odot} \cos b + \quad (7)$$

$$+r[M_{32}^- \sin l - M_{13}^- \cos l - 0.5M_{12}^+ \sin 2l \sin 2b + M_{13}^+ \cos l \cos 2b + \\ + M_{23}^+ \sin l \cos 2b - 0.5(M_{11}^+ - M_{22}^+) \cos^2 l \sin 2b + 0.5(M_{33}^+ - M_{22}^+) \sin 2b].$$

Equation (6) was obtained from Eq. (3) by adding two terms to its right-hand side,  $0.5M_{31}$  and  $0.5M_{32}$ , and subtracting them.

The system of equations (6) and (7) then becomes very convenient for its simultaneous solution. Indeed, as can be seen from Eq. (6), the two pairs of unknowns to be determined,  $M_{13}^-$  and  $M_{13}^+$ , along with  $M_{32}^-$  and  $M_{23}^+$ , have identical coefficients,  $\sin l \sin b$  and  $\cos l \sin b$ ,

respectively. In this case, the variables cannot be separated and can be found only from the simultaneous solution of the system of equations (6) and (7).

In addition, we see that one of the diagonal terms of the local deformation tensor remains uncertain. Therefore, we determine differences of the form  $(M_{11}^+ - M_{22}^+)$  and  $(M_{33}^+ - M_{22}^+)$ .

The quantities  $M_{32}^-, M_{13}^-, M_{12}^-$  are the components of the solid-body rotation vector of a small solar neighborhood around the  $x, y, z$  axes, respectively. According to our chosen rectangular coordinate system, the rotations from axis 1 to 2, from axis 2 to 3, and from axis 3 to 1 are positive.  $M_{21}^-$  is equivalent to the Oort constant  $B$ . Each of the quantities  $M_{12}^+, M_{13}^+, M_{23}^+$  describes the deformation in the corresponding plane.  $M_{12}^+$  is equivalent to the Oort constant  $A$ .

The diagonal components of the local deformation tensor  $M_{11}^+, M_{22}^+, M_{33}^+$  describe the general local contraction or expansion of the entire stellar system (divergence). The system of conditional equations (6) and (7) contain eleven unknowns to be determined by the least-squares method. In addition to the simultaneous solution of the system of equations (6) and (7), here we analyze the results of their separate solutions. In this case, Eq. (7) remains unchanged, while Eq. (6) is reduced to the form

$$\begin{aligned} 4.74r\mu_l \cos b = & X_\odot \sin l - Y_\odot \cos l + \\ & + r[M_{23} \cos l \sin b - M_{13} \sin l \sin b + M_{21}^- \cos b + M_{12}^+ \cos 2l \cos b - \\ & - 0.5(M_{11}^+ - M_{22}^+) \sin 2l \cos b], \end{aligned} \quad (8)$$

where there are only seven independent variables.

## INERTIALITY OF THE OPTICAL ICRS/HIPPARCOS SYSTEM

Table 1 presents all of the currently known results of comparing individual programs with the catalogs of the ICRS/HIPPARCOS system.

First, we will briefly describe the results, most of which were used by Kovalevsky et al. (1997) to calibrate the HIPPARCOS catalog and to estimate its residual rotation relative to the system of extragalactic sources and by Bobylev (2004b) to solve this problem.

(1) The NPM1 solution. We used the result of comparing the stellar proper motions from the NPM1 (Klemola et al. 1994) and HIPPARCOS catalogs performed by the Heidelberg group (Kovalevsky et al. 1997). This solution was obtained in the range of magnitudes  $10^m.5$ – $11^m.5$ , where (Fig. 1 in Platais et al. 1998a) the HIPPARCOS–NPM1 stellar proper motion differences have a “horizontal” pattern near zero. In our opinion, the NPM1 proper motions in this magnitude range are free from the influence of the magnitude equation, which is significant in this catalog, to the greatest extent.

(2) The NPM2 solution. The stellar proper motions from the NPM2 and HIPPARCOS catalogs were compared by Zhu (2003). However, there are no images of galaxies on NPM2 photographic plates and, hence, these proper motions are relative. Therefore, we do not

Table 1: Components of the residual rotation vector of the optical realization of the ICRS/HIPPARCOS system relative to the inertial frame of reference

Method	$P_x/P_y/P_z$	$N_\star$	$N_{area}$	$\omega_x$ , mas yr $^{-1}$	$\omega_y$ , mas yr $^{-1}$	$\omega_z$ , mas yr $^{-1}$
NPM1	10/5/16	2616	899	$-0.76 \pm 0.25$	$+0.17 \pm 0.20$	$-0.85 \pm 0.20$
NPM2	(*)	3519	347	$-0.11 \pm 0.20$	$-0.19 \pm 0.20$	$-0.75 \pm 0.28$
SPM2	22/9/28	9356	156	$+0.10 \pm 0.17$	$+0.48 \pm 0.14$	$-0.17 \pm 0.15$
Kiev	1/1/1	415	154	$-0.27 \pm 0.80$	$+0.15 \pm 0.60$	$-1.07 \pm 0.80$
Potsdam	2/1/3	256	24	$+0.22 \pm 0.52$	$+0.43 \pm 0.50$	$+0.13 \pm 0.48$
Bonn	5/3/6	88	13	$+0.16 \pm 0.34$	$-0.32 \pm 0.25$	$+0.17 \pm 0.33$
HST	0.1/0.1/0.05	78		$-1.60 \pm 2.87$	$-1.92 \pm 1.54$	$+2.26 \pm 3.42$
EOP	8/2/—			$-0.93 \pm 0.28$	$-0.32 \pm 0.28$	—
PUL2	3/1/4	1004	147	$-0.98 \pm 0.47$	$-0.03 \pm 0.38$	$-1.66 \pm 0.42$
XPM	28/9/33	$1 \times 10^6$	1431	$-0.06 \pm 0.15$	$+0.17 \pm 0.14$	$-0.84 \pm 0.14$
VLBI-07	6/1/5	46		$-0.55 \pm 0.34$	$-0.02 \pm 0.36$	$+0.41 \pm 0.37$
Minor Pl	25/5/6	116		$+0.12 \pm 0.08$	$+0.66 \pm 0.09$	$-0.56 \pm 0.16$
Mean 1				$-0.22 \pm 0.19$	$+0.14 \pm 0.10$	$-0.49 \pm 0.23$
Mean 2				$-0.11 \pm 0.14$	$+0.24 \pm 0.10$	$-0.52 \pm 0.16$

Note. (\*)—the NPM2 solution is not used,  $N_\star$  is the number of stars/asteroids,  $N_{area}$  is the number of areas on the celestial sphere, mean 1 is a simple mean (without HST), mean 2 is a weighted mean.

use this solution to derive the mean values of  $\omega_x, \omega_y, \omega_z$ . It is given in Table 1 to emphasize its similarity to the NPM1 solution.

(3) The SPM2 solution. The stellar proper motions from the SPM2 (Platais et al. 1998b) and HIPPARCOS catalogs were compared by Zhu (2001).

(4) The PUL2 solution. The parameters  $\omega_x, \omega_y, \omega_z$  were found by comparing the Pulkovo PUL2 photographic catalog (Bobylov et al. 2004) and HIPPARCOS.

(5) The KIEV solution. The stellar proper motions from the GPM1 (Rybka and Yatsenko 1997) and HIPPARCOS catalogs were compared by Kislyuk et al. (1997).

(6) The POTSDAM solution. The parameters  $\omega_x, \omega_y, \omega_z$  of the Potsdam program were taken from Hirte et al. (1996).

(7) The BONN solution. The results of the Bonn program are presented in Geffert et al. (1997) and Tucholke et al. (1997).

(8) The EOP solution. The results of the analysis of Earth orientation parameters (EOP) were taken from Vondrák et al. (1997). Only two rotation parameters,  $\omega_x$ , and  $\omega_y$  are determined in this method.

(9) The HST solution. The results of stellar observations with the Hubble Space Telescope (HST) were taken from Hemenway et al. (1997).

Now, we will point out several new results that have not been used previously to solve this problem.



(10) The XPM solution. The XPM catalog (Fedorov et al., 2009) contains absolute proper motions for about 275 million stars fainter than 12m derived by comparing their positions in the 2MASS and USNO-A2.0 (Monet 1998) catalogs. The absolutization was made using about 1.5 million galaxies from the 2MASS catalog of extended sources. Thus, the XPM catalog is an independent realization of the inertial frame of reference. The stellar proper motions from the XPM and UCAC2 (Zacharias et al. 2004) catalogs were compared by Bobylev et al. (2010). The parameters  $\omega_x, \omega_y, \omega_z$  were calculated using about 1 million stars. Among all of the programs listed in Table 1, the XPM solution is unique in that it was obtained from the differences of stars covering the entire sky almost completely, except for the zone  $\delta > 54^\circ$ , where there are no UCAC2 stars.

(11) The VLBI-07 solution. Boboltz et al. (2007) analyzed the positions and proper motions of 46 radio stars and obtained new parameters of the mutual orientation of the optical realization (HIPPARCOS) and the radio system.

(12) The “MINOR PLANETS” solution. Chernetenko (2008) estimated the rotation parameters of the HIPPARCOS system relative to the DE403 and DE405 coordinate systems of ephemerides by analyzing a long-term series of asteroid observations. This result suggests that either the dynamical DE403 and DE405 theories need to be improved or the HIPPARCOS system needs to be corrected. We reduced the weight of this solution by half because of the possible contribution from the inaccuracy of the dynamical DE403 and DE405 theories.

The weight of each of the comparison catalogs was taken to be inversely proportional to the square of the random error  $e_\omega$  in the corresponding quantities  $\omega_x, \omega_y, \omega_z$  and was calculated from the formula

$$P_i = e_{kiev}^2 / e_i^2, \quad i = 1, \dots, 11. \quad (9)$$

Not all of the authors use the equations to determine  $\omega_x, \omega_y, \omega_z$  in the form in which they were suggested by Lindegren and Kovalevsky (1995):

$$\Delta\mu_\alpha \cos \delta = \omega_x \cos \alpha \sin \delta + \omega_y \sin \alpha \sin \delta - \omega_z \cos \delta, \quad (10)$$

$$\Delta\mu_\delta = -\omega_x \sin \alpha + \omega_y \cos \alpha, \quad (11)$$

where the catalog–HIPPARCOS differences are on the left-hand sides of the equations. Therefore, in several cases, the signs of the quoted quantities were reduced to the necessary uniform form (Zhu 2001, 2003; Boboltz et al. 2007).

The last rows of Table 1 give Mean 1 calculated as a simple mean and Mean 2 that was calculated as a weighted mean and is the main result of our analysis.

Denote the components of the rotation vector around the rectangular equatorial axes by  $\omega_x, \omega_y, \omega_z$ ; then,

$$\begin{pmatrix} \Omega_x \\ \Omega_y \\ \Omega_z \end{pmatrix} = \mathbf{G} \begin{pmatrix} M_{32}^- \\ M_{13}^- \\ M_{21}^- \end{pmatrix} + 4.74 \begin{pmatrix} \omega_x \\ \omega_y \\ -\omega_z \end{pmatrix}, \quad (12)$$

where

$$\mathbf{G} = \begin{pmatrix} -0.0548 & +0.4941 & -0.8677 \\ -0.8734 & -0.4448 & -0.1981 \\ -0.4838 & +0.7470 & +0.4560 \end{pmatrix} \quad (13)$$

is the well-known transformation matrix between the unit vectors of the Galactic and equatorial coordinate systems. From Eqs. (9) and (10), it is easy to see the relationship between  $M_{13}^-$  and  $\omega_z$ . Assuming the components in the mean-2 solution to be zero,

$$\begin{pmatrix} \Omega_x \\ \Omega_y \\ \Omega_z \end{pmatrix} = \mathbf{G} \begin{pmatrix} M_{32}^- \\ M_{13}^- \\ M_{21}^- \end{pmatrix} + 4.74 \begin{pmatrix} 0 \\ 0 \\ 0.52 \end{pmatrix}, \quad (14)$$

for the case where the left- and right-hand sides are expressed in  $\text{km s}^{-1} \text{ kpc}^{-1}$ .

## KINEMATICS OF THE DISK WARP

The results of determining the kinematic parameters of the Ogorodnikov–Milne model using a sample of RGC stars derived by simultaneously solving the system of equations (6) and (7) are presented in Table 2. The second column gives the solution obtained without applying any corrections to the input data; the third column gives the solution for the case where the stellar proper motions in the form  $\mu_\alpha \cos \delta$  were corrected by applying the correction  $\omega_z = -0.52 \text{ mas yr}^{-1}$  (14) using Eq. (10).

The parameters derived by separately solving Eqs. (8) and (7) are presented in Table 3.

As can be seen from Table 2, applying the correction affected only three components of the rotation tensor: insignificantly  $M_{21}^-$ , noticeably  $M_{32}^-$ , and most strongly  $M_{13}^-$ , which is explained by the structure of the matrix  $\mathbf{G}$  (13). Since the components  $M_{13}^-$  and  $M_{13}^+$  found (the third column of Table 2) do not differ significantly from zero, they may be set equal to zero.

Suppose that the values of  $M_{21}^-$  and  $M_{21}^+$  (the Oort constants) found describe only the rotation around the Galactic  $z$  axis, while the motion in the  $yz$  plane is independent. Let us now consider the displacement tensor  $M_W$  that describes the kinematics in the  $yz$  plane:

$$M_W = \begin{pmatrix} M_{22} & M_{23} \\ M_{32} & M_{33} \end{pmatrix} = \begin{pmatrix} \frac{\partial u_2}{\partial r_2} & \frac{\partial u_2}{\partial r_3} \\ \frac{\partial u_3}{\partial r_2} & \frac{\partial u_3}{\partial r_3} \end{pmatrix}. \quad (15)$$

As has already been noted, when using only the stellar proper motions, we can determine only the difference  $(M_{33}^+ - M_{22}^+)$ . The identity  $(M_{33}^+ - M_{22}^+) \equiv (M_{33} - M_{22})$  is valid for the diagonal elements. As can be seen from Table 2, the value of this quantity differs significantly from zero.

Three cases are possible when analyzing tensor (15):

- 1)  $M_{22} \neq 0, M_{33} = 0$ ;
- 2)  $M_{22} = 0, M_{33} \neq 0$ ;
- 3)  $M_{22} = 0, M_{33} = 0$ .

For the completeness of the picture, note that case 4 is also possible:  $M_{22} \neq 0, M_{33} \neq 0$ ; since this requires data on the stellar radial velocities, this case is not considered here.

Consider case 1,  $M_{33} = 0$ , using the data from the third column of Table 2,  $M_{22} = 1.3 \pm 0.4 \text{ km s}^{-1} \text{ kpc}^{-1}$ . The components of the displacement tensor  $M_W$ , the symmetric deformation tensor  $M_W^+$ , and the antisymmetric rotation tensor  $M_W^-$  are ( $\text{km s}^{-1} \text{ kpc}^{-1}$ )

$$M_W = \begin{pmatrix} 1.3_{(0.4)} & 3.6_{(0.3)} \\ -1.6_{(0.3)} & 0 \end{pmatrix}, \quad (16)$$

$$M_W^+ = \begin{pmatrix} 1.3_{(0.4)} & 1.0_{(0.2)} \\ 1.0_{(0.2)} & 0 \end{pmatrix}, \quad (17)$$

$$M_W^- = \begin{pmatrix} 0 & -2.6_{(0.2)} \\ -2.6_{(0.2)} & 0 \end{pmatrix}. \quad (18)$$

The deformation tensor  $M_W^+$  in the principal axes is ( $\text{km s}^{-1} \text{ kpc}^{-1}$ ):

$$\begin{aligned} M_W^+ &= \begin{pmatrix} \lambda_1 & 0 \\ 0 & \lambda_2 \end{pmatrix} = \\ &= \begin{pmatrix} 1.8 & 0 \\ 0 & -0.5 \end{pmatrix}, \end{aligned}$$

and the angle between the positive direction of the  $0y$  axis and the first principal axis of this ellipse is  $29 \pm 6^\circ$ .

Equation (1) can be written as

$$\mathbf{V} = \mathbf{V}_o + \text{grad } F + (\boldsymbol{\omega} \times \mathbf{r}).$$

Analysis of  $\text{grad } F$  shows (Sedov 1970) that an infinitesimal sphere of radius  $r$  composed of points of the medium at time  $t$ ,

$$x^2 + y^2 + z^2 = r^2$$

transforms into a deformation ellipsoid after time  $\Delta t$ ,

$$\frac{x^{*2}}{(1 + \lambda_1 \Delta t)^2} + \frac{y^{*2}}{(1 + \lambda_2 \Delta t)^2} + \frac{z^{*2}}{(1 + \lambda_3 \Delta t)^2} = r^2,$$

which is shown in Fig. 2b for our two-dimensional case.

For case 2, we have  $M_{33} = -1.3 \pm 0.4 \text{ km s}^{-1} \text{ kpc}^{-1}$  and  $M_{22} = 0$ . The deformation tensor  $M_W^+$  in the principal axes is ( $\text{km s}^{-1} \text{ kpc}^{-1}$ )

$$M_W^+ = \begin{pmatrix} 0.5 & 0 \\ 0 & -1.8 \end{pmatrix},$$

Table 2: Kinematic parameters of the Ogorodnikov–Milne model found by simultaneously solving the system of equations (6) and (7)

Parameter	Without correction	With correction
$X_{\odot}$	$7.99 \pm 0.10$	$7.99 \pm 0.10$
$Y_{\odot}$	$16.40 \pm 0.10$	$16.40 \pm 0.10$
$Z_{\odot}$	$6.72 \pm 0.09$	$6.72 \pm 0.09$
$A = M_{21}^+$	$15.82 \pm 0.21$	$15.82 \pm 0.21$
$M_{32}^-$	$-1.40 \pm 0.18$	$-2.60 \pm 0.18$
$M_{13}^-$	$-1.99 \pm 0.18$	$-0.15 \pm 0.18$
$B = M_{21}^-$	$-11.99 \pm 0.15$	$-10.87 \pm 0.15$
$M_{11-22}^+$	$-7.75 \pm 0.39$	$-7.75 \pm 0.39$
$M_{13}^+$	$-0.47 \pm 0.23$	$-0.47 \pm 0.23$
$M_{23}^+$	$1.00 \pm 0.22$	$1.00 \pm 0.22$
$M_{33-22}^+$	$-1.26 \pm 0.44$	$-1.26 \pm 0.44$

Note:  $X_{\odot}, Y_{\odot}, Z_{\odot}$  in  $\text{km s}^{-1}$ , other parameters in  $\text{km s}^{-1} \text{ kpc}^{-1}$ .

Table 3: Kinematic parameters of the Ogorodnikov–Milne model found by separately solving Eqs. (8) and (7)

Parameter	Without correction <sup>a</sup>	With correction <sup>a</sup>	Without correction <sup>b</sup>	With correction <sup>b</sup>
$X_{\odot}$	$7.89 \pm 0.12$	$7.89 \pm 0.12$	$8.51 \pm 0.21$	$8.51 \pm 0.21$
$Y_{\odot}$	$16.13 \pm 0.13$	$16.13 \pm 0.13$	$17.40 \pm 0.21$	$17.40 \pm 0.21$
$Z_{\odot}$	—	—	$6.73 \pm 0.08$	$6.73 \pm 0.08$
$A = M_{21}^+$	$15.76 \pm 0.25$	$15.76 \pm 0.25$	$15.99 \pm 0.48$	$15.99 \pm 0.48$
$M_{32}^-$	—	—	$-1.47 \pm 0.25$	$-2.66 \pm 0.25$
$M_{13}^-$	—	—	$-1.46 \pm 0.25$	$0.38 \pm 0.25$
$B = M_{21}^-$	$-12.02 \pm 0.17$	$-10.91 \pm 0.17$	—	—
$M_{11-22}^+$	$-8.21 \pm 0.46$	$-8.21 \pm 0.46$	$-4.31 \pm 1.03$	$-4.31 \pm 1.03$
$M_{13}^+$	—	—	$0.17 \pm 0.34$	$0.17 \pm 0.34$
$M_{23}^+$	—	—	$1.11 \pm 0.32$	$1.11 \pm 0.32$
$M_{33-22}^+$	—	—	$0.29 \pm 0.59$	$0.29 \pm 0.59$
$M_{23}$	$2.24 \pm 0.46$	$3.43 \pm 0.46$	—	—
$M_{13}$	$-2.93 \pm 0.43$	$-1.09 \pm 0.43$	—	—

<sup>a</sup>The parameters were found by solving Eq. (8).

<sup>b</sup>The parameters were found by solving Eq. (7).

Note:  $X_{\odot}, Y_{\odot}, Z_{\odot}$  in  $\text{km s}^{-1}$ , other parameters in  $\text{km s}^{-1} \text{ kpc}^{-1}$ .

the angle between the positive direction of the  $0y$  axis and the first principal axis of this ellipse is  $29 \pm 6^\circ$ .

For case 3, where  $M_{33} = 0$  and  $M_{22} = 0$ , the deformation tensor  $M_W^+$  has two roots:  $\lambda_1 = 1.0 \text{ km s}^{-1} \text{ kpc}^{-1}$  and  $\lambda_2 = -1.0 \text{ km s}^{-1} \text{ kpc}^{-1}$ ; therefore, the first principal axis of this ellipse is oriented at an angle of  $45^\circ$  to the  $0y$  axis.

In all three cases, the divergence  $0.5(M_{22} + M_{33})$  is insignificant. It is  $+0.6 \pm 0.4$ , and  $0 \text{ km s}^{-1} \text{ kpc}^{-1}$  for the first, second, and third cases, respectively.

As a result, we can conclude that the kinematics in the  $yz$  plane can be described as a rotation around the Galactic  $x$  axis with an angular velocity  $\Omega_W = M_{32}^- - \lambda_1$ . This angular velocity is  $-4.4 \pm 0.5$ ,  $-3.1 \pm 0.5$ , and  $-3.6 \pm 0.3 \text{ km s}^{-1} \text{ kpc}^{-1}$  for the first, second, and third cases, respectively.

Let us estimate the linear velocities in the  $yz$  plane. The mean photometric distance for our sample of RGC stars is  $\bar{r} = 0.57 \pm 0.17 \text{ kpc}$ . The linear solidbody rotation velocity is then  $M_{32}^- \cdot \bar{r} = -1.5 \pm 0.1 \text{ km s}^{-1}$ . The maximum deformation velocity is  $\lambda_1 \cdot \bar{r} = 1.0 \pm 0.3 \text{ km s}^{-1}$  and the highest (among the cases considered) linear velocity is  $\Omega_W \cdot \bar{r} = -2.5 \pm 0.3 \text{ km s}^{-1}$ .

Figure 2 gives a qualitative picture that reflects the pattern of our results. The distribution of rotation velocity vectors in the  $yz$  plane for the case of rotation we found is shown in Fig. 2a. Figure 2b shows how a circumference of unit radius turns into a deformation ellipse after a unit time interval.

According to the results of our separate solution of Eqs. (8) and (7) (the third and fifth columns of Table 3), for example, for case 1, we have

$$M_W = \begin{pmatrix} -0.3_{(0.6)} & 3.8_{(0.5)} \\ -1.6_{(0.4)} & 0 \end{pmatrix}, \quad (19)$$

$$M_W^+ = \begin{pmatrix} -0.3_{(0.6)} & 1.1_{(0.3)} \\ 1.1_{(0.3)} & 0 \end{pmatrix}, \quad (20)$$

$$M_W^- = \begin{pmatrix} 0 & -2.7_{(0.3)} \\ -2.7_{(0.3)} & 0 \end{pmatrix}. \quad (21)$$

We can see from our comparison of matrixes (19) and (16), (20) and (17), (21) and (18) that there are differences only in the diagonal element. This leads us to conclude that both approaches used (the simultaneous and separate solution of the equations) are equivalent, because they yield coincident results.

When writing Eq. (14), we set the components equal to zero,  $\omega_x = 0$  and  $\omega_y = 0$ . As we see from the Mean 2 solution in Table 1, the value of the component  $\omega_y$  was found to be nonzero outside the  $2\sigma$  range. However, the kinematic parameters calculated by taking this into account, i.e.,  $\omega_y \neq 0$  and  $\omega_z \neq 0$ , have no significant differences between the solutions reflected in Tables 2 and 3 and, hence, we do not give them.

## DISCUSSION

Drimmel et al. (2000) provide arguments for the model of precession of the warped disk in the  $zx$  plane (rotation around the  $y$  axis) with an angular velocity of  $-25 \text{ km s}^{-1} \text{ kpc}^{-1}$ .

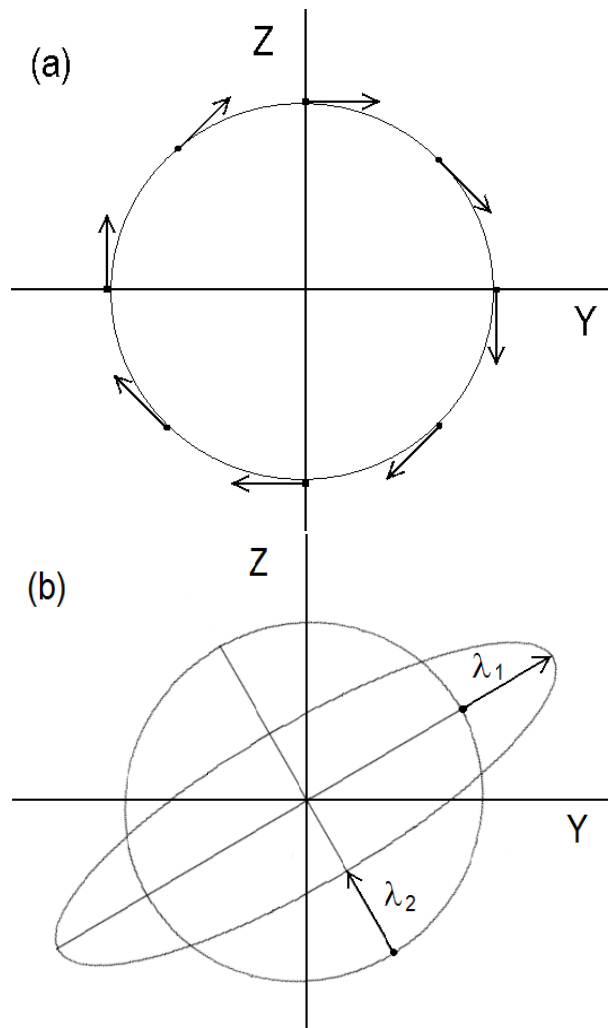


Fig. 2. Distribution of rotation velocity vectors (a) and deformation velocity vectors (b) in the  $yz$  plane.

However, as can be seen from Table 2, as a result of applying the correction  $\omega_z = -0.52$  mas yr<sup>-1</sup>, the component of the rotation tensor around the  $y$  axis ( $M_{13}^-$ ) has an almost zero value and the component of the deformation tensor in this plane ( $M_{13}^+$ ) does not differ significantly from zero.

The angular velocity  $\Omega_W$  estimated here is inconsistent with the analysis of the motion of giants of various spectral types (O–M) performed by Miyamoto et al. (1993), who found a positive direction of rotation around the  $x$  axis (directed toward the Galactic center). Note that the analyzed stellar proper motions were determined in the FK5 (Fundamental Catalog 5) system, which is noticeably distorted by the uncertainty in the precession constant. On the other hand, having analyzed the proper motions of O–B5 stars in the HIPPARCOS system, Miyamoto and Zhu (1998) also reached the conclusion about a positive rotation around the  $x$  axis.

At present, it is impossible to choose between the three forms of the deformation tensor considered in the previous section due to the absence of data on stellar radial velocities and distances. Note that based on a sample of 3632 relatively close RGC stars with known HIPPARCOS trigonometric parallaxes and radial velocities, we estimated the parameters  $M_{22} = -1.3 \pm 3.2$  km s<sup>-1</sup> kpc<sup>-1</sup> and  $M_{33} = -1.1 \pm 2.6$  km s<sup>-1</sup> kpc<sup>-1</sup> (Bobylev et al. 2009). Consequently, the difference ( $M_{33}^+ - M_{22}^+$ ) is very close to zero and, hence, the orientation of the deformation ellipse is close to 45°, as in case 3 considered.

In the Introduction, we listed various hypotheses about the nature of the Galactic disk warp. In our opinion, the hypothesis about an outflow of gas from the Magellanic Clouds (Olano 2004) has been worked out in greatest detail. Assuming the distance to the Large Magellanic Cloud to be  $r_{LMC} = 50$  kpc, we find that the linear velocity of the rotation we revealed at this distance,  $(-3.1 \pm 0.5) \leq \Omega_W \leq (-4.4 \pm 0.5)$  km s<sup>-1</sup> kpc<sup>-1</sup>, is  $|\Omega_W| \cdot r_{LMC} = (155 \div 220) \pm 25$  km s<sup>-1</sup>. Such velocities are in agreement with the estimate of the motion of high-velocity hydrogen clouds relative to the local standard of rest,  $\approx 200$  km s<sup>-1</sup> (Olano 2004), and the rotation direction we found is in good agreement with the direction of motion of the Magellanic Clouds around the Galaxy during the past 570 Myr (Fig. 6 from Olano 2004).

## CONCLUSIONS

We analyzed the kinematics of about 82000 RGC stars from the Tycho-2 catalog. These stars are a variety of “standard candles”, because they occupy a compact region on the Hertzsprung-Russell diagram. Therefore, photometric distance estimates with an accuracy of at least 30% are available for them. The RGC stars considered lie in the range of heliocentric distances  $0.3 \text{ kpc} < d < 1 \text{ kpc}$ .

Since these stars are distributed fairly uniformly in space, they are of great interest not only in studying the Galaxy’s general rotation described by the rotation parameters in the Galactic  $xy$  plane but also in the other two planes, namely  $yz$  and  $zx$ .

For a reliable description of their kinematic peculiarities, we should be confident that the observational data (Tycho-2 proper motions) are free from the systematic errors related to the referencing of the optical realization of the ICRS/HIPPARCOS system to the

inertial frame of reference specified by extragalactic sources.

Here, we gave much attention to this problem. Based on all of the currently available data, we determined new, most probable components of the residual rotation vector of the optical realization of the ICRS/HIPPARCOS system relative to the inertial frame of reference,  $(\omega_x, \omega_y, \omega_z) = (-0.11, 0.24, -0.52) \pm (0.14, 0.10, 0.16) \text{ mas yr}^{-1}$ . This led us to conclude that a small correction,  $\omega_z = -0.52 \text{ mas yr}^{-1}$ , should be applied to the Tycho-2 stellar proper motions of the form  $\mu_\alpha \cos \delta$ .

By applying this correction, we showed that, apart from their involvement in the general Galactic rotation described by the Oort constants  $A = 15.8 \pm 0.2 \text{ km s}^{-1} \text{ kpc}^{-1}$  and  $B = -10.9 \pm 0.2 \text{ km s}^{-1} \text{ kpc}^{-1}$ , the RGC stars considered have peculiarities in the  $yz$  plane related, in our opinion, to the kinematics of the warped Galactic stellar-gaseous disk.

The component of the solid-body rotation of the local solar neighborhood around the Galactic  $x$  axis is  $M_{32}^- = -2.6 \pm 0.2 \text{ km s}^{-1} \text{ kpc}^{-1}$ . The parameter of the deformation tensor in this plane  $M_{23}^+ = 1.0 \pm 0.2 \text{ km s}^{-1} \text{ kpc}^{-1}$  and the difference  $M_{33} - M_{22} = -1.3 \pm 0.4 \text{ km s}^{-1} \text{ kpc}^{-1}$  differ significantly from zero.

On the whole, the kinematics of the warped Galactic stellar-gaseous disk in the local solar neighborhood can be described as a rotation around the Galactic  $x$  axis directed from the Sun toward the Galactic center with an angular velocity  $(-3.1 \pm 0.5) \leq \Omega_W \leq (-4.4 \pm 0.5) \text{ km s}^{-1} \text{ kpc}^{-1}$ . Thus, the rotation is around an axis close to the line of nodes of this structure. In the case where the difference  $M_{33} - M_{22}$  may be set equal to zero, the angular velocity  $\Omega_W$  is  $-3.6 \pm 0.3 \text{ km s}^{-1} \text{ kpc}^{-1}$ . If  $M_{22} = 0$  and  $M_{33} \neq 0$ , then  $\Omega_W = -3.1 \pm 0.5 \text{ km s}^{-1} \text{ kpc}^{-1}$ . If  $M_{22} \neq 0$  and  $M_{33} = 0$ , then  $\Omega_W$  reaches  $-4.4 \pm 0.5 \text{ km s}^{-1} \text{ kpc}^{-1}$ .

## ACKNOWLEDGMENTS

I am grateful to the referees for helpful remarks that contributed to an improvement of the paper and to A.T. Bajkova for her help in the work. This study was supported by the Russian Foundation for Basic Research (project nos. 08-02-00400 and 09-02-90443-Ukr-f) and, in part, by the “Origin and Evolution of Stars and Galaxies” Program of the Presidium of the Russian Academy of Sciences.

## REFERENCES

1. J. Bailin, *Astrophys. J.* 583, L79 (2003).
2. E. Battaner, E. Florido, and M.L. Sanchez-Saavedra, *Astron. Astrophys.* 236, 1 (1990).
3. D.A. Boboltz, A.L. Fey, W.K. Puatua, et al., *Astron. J.* 133, 906 (2007).
4. V.V. Bobylev, *Pis'ma Astron. Zh.* 30, 289 (2004a) [*Astron. Lett.* 30, 251 (2004)].
5. V.V. Bobylev, *Pis'ma Astron. Zh.* 30, 930 (2004b) [*Astron. Lett.* 30, 848 (2004)].
6. V.V. Bobylev, N.M. Bronnikova, and N.A. Shakht, *Pis'ma Astron. Zh.* 30, 519 (2004) [*Astron. Lett.* 30, 469 (2004)].



7. V.V. Bobylev, A.S. Stepanishchev, A.T. Bajkova, and G.A. Gontcharov, *Pis'ma Astron. Zh.* 35, 920 (2009) [*Astron. Lett.* 35, 836 (2009)].
8. V.V. Bobylev, P.N. Fedorov, A.T. Bajkova, and V.S. Akhmetov, *Pis'ma Astron. Zh.* 36, 535 (2010) [*Astron. Lett.* 36, 506 (2010)].
9. W.B. Burton, *Galactic and Extragalactic Radio Astronomy*, Ed. by G. Verschuur and K. Kellerman (Springer, New York, 1988), p. 295.
10. J.C. Cersosimo, S. Mader, N. Santiago Figueroa, et al., *Astrophys. J.* 699, 469 (2009).
11. Yu.A. Chernetenko, *Pis'ma Astron. Zh.* 34, 296 (2008) [*Astron. Lett.* 34, 266 (2008)].
12. S.V.M. Clube, *Mon. Not. R. Astron. Soc.* 159, 289 (1972).
13. S.V.M. Clube, *Mon. Not. R. Astron. Soc.* 161, 445 (1973).
14. W. Dehnen, *Astron. J.* 115, 2384 (1998).
15. R. Drimmel and D.N. Spergel, *Astrophys. J.* 556, 181 (2001).
16. R. Drimmel, R.L. Smart, and M.G. Lattanzi, *Astron. Astrophys.* 354, 67 (2000).
17. P.N. Fedorov, A.A. Myznikov, and V.S. Akhmetov, *Mon. Not. R. Astron. Soc.* 393, 133 (2009).
18. M. Geffert, A.R. Klemola, M. Hiesgen, et al., *Astron. Astrophys.* 124, 157 (1997).
19. G.A. Gontcharov, *Pis'ma Astron. Zh.* 34, 868 (2008) [*Astron. Lett.* 34, 785 (2008)].
20. P.D. Hemenway, R.L. Duncombe, E.P. Bozayan, et al., *Astron. J.* 114, 2796 (1997).
21. *The HIPPARCOS and Tycho Catalogues*, ESA SP-1200 (1997).
22. S. Hirte, E. Schilbach, and R.-D. Scholz, *Astron. Astrophys. Suppl. Ser.* 126, 31 (1996).
23. E. Hog, C. Fabricius, V.V. Makarov, et al., *Astron. Astrophys.* 355, L27 (2000).
24. P.M.W. Kalberla and L. Dedes, *Astron. Astrophys.* 487, 951 (2008).
25. V.S. Kislyuk, SP. Rybka, A.I. Yatsenko, et al., *Astron. Astrophys.* 321, 660 (1997).
26. A.R. Klemola, R.B. Hanson, and B.F. Jones, in *Galactic and Solar System Optical Astrometry*, Ed. by L.V. Morrison and G.F. Gilmore (Cambridge Univ., Cambridge, 1994), p. 20.
27. J. Kovalevsky, L. Lindegren, M.A.C. Perryman, et al., *Astron. Astrophys.* 323, 620 (1997).
28. L. Lindegren and J. Kovalevsky, *Astron. Astrophys.* 304, 189 (1995).
29. M. López-Corredoira, J. Betancort-Rijo, and J. Beckman, *Astron. Astrophys.* 386, 169 (2002).
30. C. Ma, E.F. Arias, T.M. Eubanks, et al., *Astron. J.* 116, 516 (1998).
31. M. Miyamoto and Z. Zhu, *Astron. J.* 115, 1483 (1998).
32. M. Miyamoto, M. Sôma, and M. Yoshizawa, *Astron. J.* 105, 2138 (1993).
33. Y. Momany, S. Zaggia, G. Gilmore, et al., *Astron. Astrophys.* 451, 515 (2006).
34. D.G. Monet, *Bull. Am. Astron. Soc.* 30, 1427 (1998).
35. K.F. Ogorodnikov, *Dynamics of Stellar Systems* (Fizmatgiz, Moscow, 1965) [in Russian].

36. C.A. Olano, *Astron. Astrophys.* 423, 895 (2004).
37. I. Platais, V. Kozhurina-Platais, T.M. Girard, et al., *Astron. Astrophys.* 331, 1119 (1998a).
38. I. Platais, T.M. Girard, V. Kozhurina-Platais, et al., *Astron. J.* 116, 2556 (1998b).
39. S.P. Rybka, *Kinem Fiz. Neb. Tel* 22, 225 (2006).
40. S.P. Rybka and A.I. Yatsenko, *Astron. Astrophys. Suppl. Ser.* 121, 243 (1997).
41. L.I. Sedov, *Mechanics of Continuous Media* (Nauka, Moscow, 1970), Vol. 1 [in Russian].
42. M.F. Skrutskie, R.M. Cutri, R. Stiening, et al., *Astron. J.* 131, 1163 (2006).
43. L. Sparke and S. Casertano, *Mon. Not. R. Astron. Soc.* 234, 873 (1988).
44. H.-J. Tucholke, P. Brosche, and M. Odenkirchen, *Astron. Astrophys. Suppl. Ser.* 124, 157 (1997).
45. V.V. Vityazev and A.S. Tsvetkov, *Pis'ma Astron. Zh.* 35, 114 (2009) [*Astron. Lett.* 35, 100 (2009)].
46. J. Vondrák, C. Ron, I. Pešek, *Astron. Astrophys.* 319, 1020 (1997).
47. G. Westerhout, *Bull. Astron. Inst. Netherlands* 13, 201 (1957).
48. S.K. Yi, Y.-C. Kim, and P. Demarque, *Astrophys. J. Suppl. Ser.* 144, 259 (2003).
49. I. Yusifov, *astro-ph/0405517* (2004).
50. N. Zacharias, S.E. Urban, M.I. Zacharias, et al., *Astron. J.* 127, 3043 (2004).
51. Zi Zhu, *Publ. Astron. Soc. Jpn.* 53, L33 (2001).
52. Zi Zhu, in *JOURNEÉS-2003, Astrometry, Geodynamics and Solar System Dynamics: From Milliarcseconds to Microarcseconds*, Ed. by N. Capitaine (Observ. de Paris, Paris, 2003), p. 95.

Translated by N. Samus'